Kinetic simulations of high-Mach number nonrelativistic shocks - status and challenges

Jacek Niemiec

Institute of Nuclear Physics, Polish Academy of Sciences, Kraków, Poland

Collaborators:
Martin Pohl, Volkmar Wieland, Iman Rafighi - University of Potsdam, Germany
Artem Bohdan, Oleh Kobzar - INP PAS, Kraków, Poland
Ken-Ichi Nishikawa - University of Alabama in Huntsville, USA

Astrophysical Shocks, AIP, Potsdam, March 5-7, 2018

Introduction

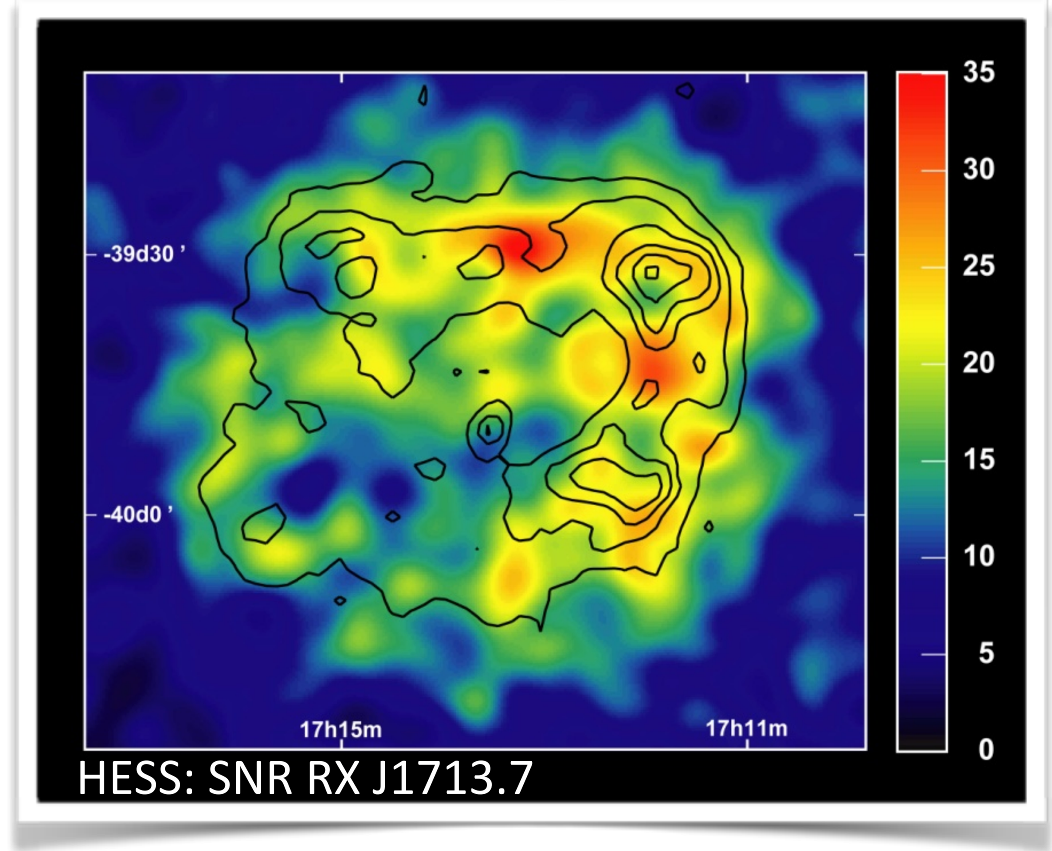

Diffusive Shock Acceleration (DSA) process assumed to work at nonrelativistic shocks of young SNRs and provide the main part of Galactic cosmic-ray flux.

Today's topic:

nonrelativistic perpendicular high Mach number collisionless shocks

- nonlinear shock structure
- cyclic shock self-reformation
- shock rippling
- electron injection

young SNR connection (M_A~10-150, β <1)

Wieland et al. 2016, ApJ, 820:62
Bohdan et al., 2017, ApJ, 847:71

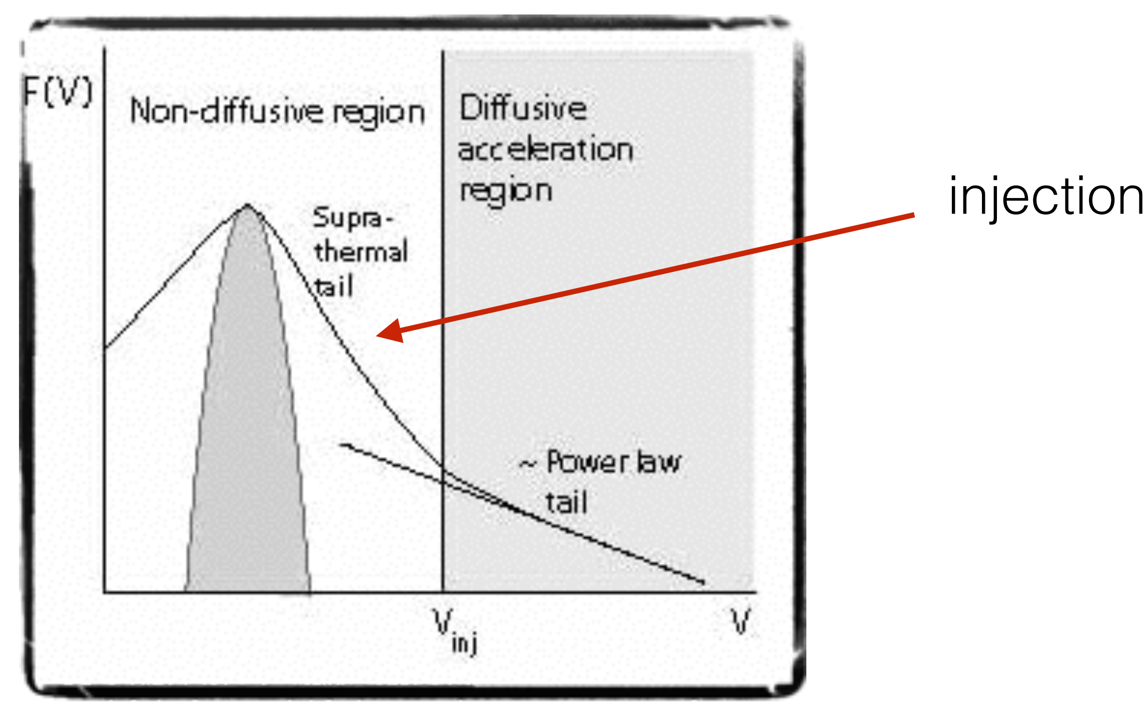

Method of Particle-In-Cell Simulations

- Fully self-consistent description of collisionless plasma:
  - Vlasov equation (kinetic theory; time evolution of particle distribution function $f(\mathbf{x},\mathbf{v},t)$ in phase-space) + Maxwell's equations
- Particle-In-Cell modeling - an *ab-initio* method of Vlasov equation solution through:
  - integration of Maxwell's equations on a numerical grid
  - integration of relativistic particle equations of motion in collective self-consistent EM field

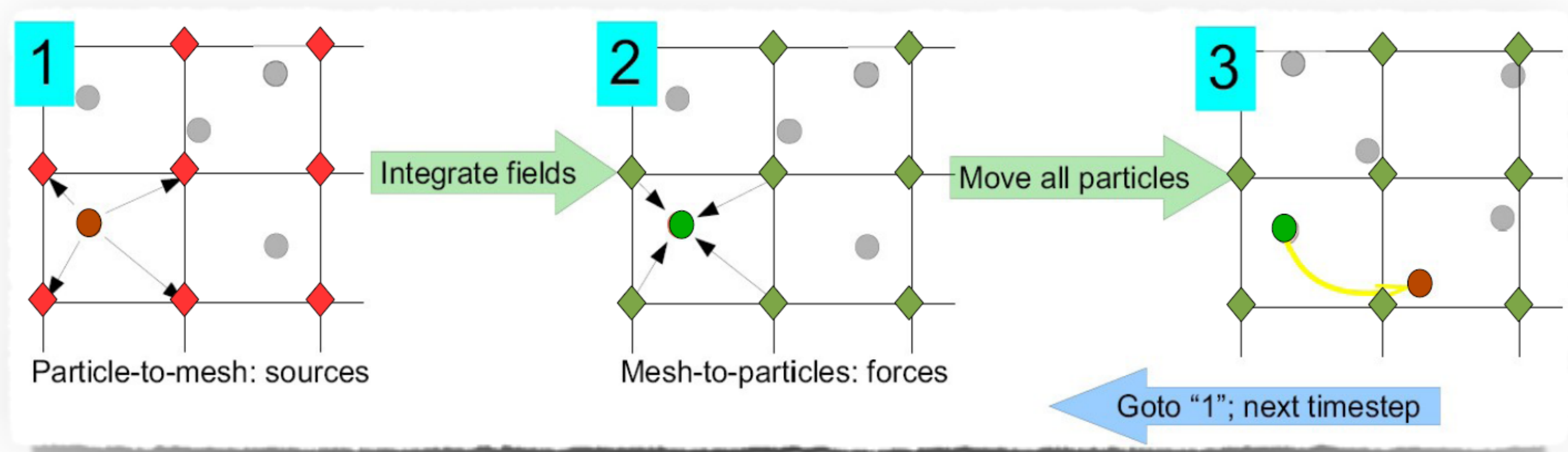

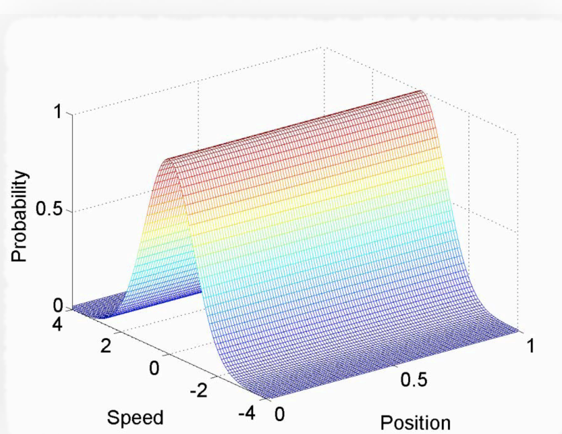

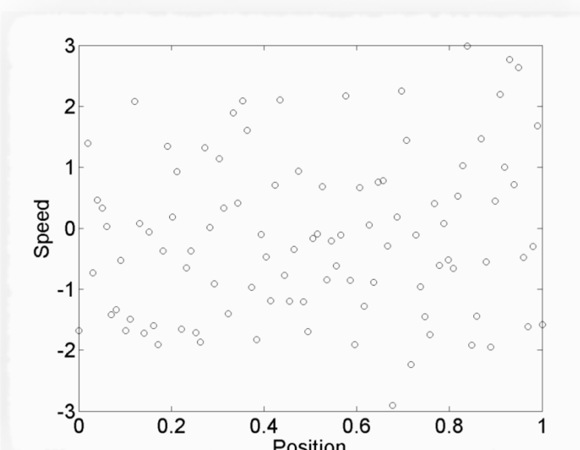

Particle distribution function represented by macroparticles on a numerical grid.
(Macroparticles represent a small volume of particle phase-space; equations of motion as for realistic particles)

PIC Numerical Model

Definition of plasma: $L \gg \lambda_D$

Typical astrophysical system $N_D >> 1$ (e.g. ionosphere $N_D \sim 10^4$)

Basic plasma condition: $\frac{\langle E_{kin} \rangle}{\langle E_{pot} \rangle} \gg 1$

$$\frac{\langle E_{kin} \rangle}{\langle E_{pot} \rangle} \sim 6\pi N_D^{2/3}$$

Is $N_D \sim 10$ *enough*? How else obtain $N_D \gg 1$?

$$\frac{\nu_c}{\omega_{pe}} \sim \frac{1}{N_D} \ln N_D$$

- numerical grid for EM fields
- finite-size particle shape model - effective elimination of short-range forces

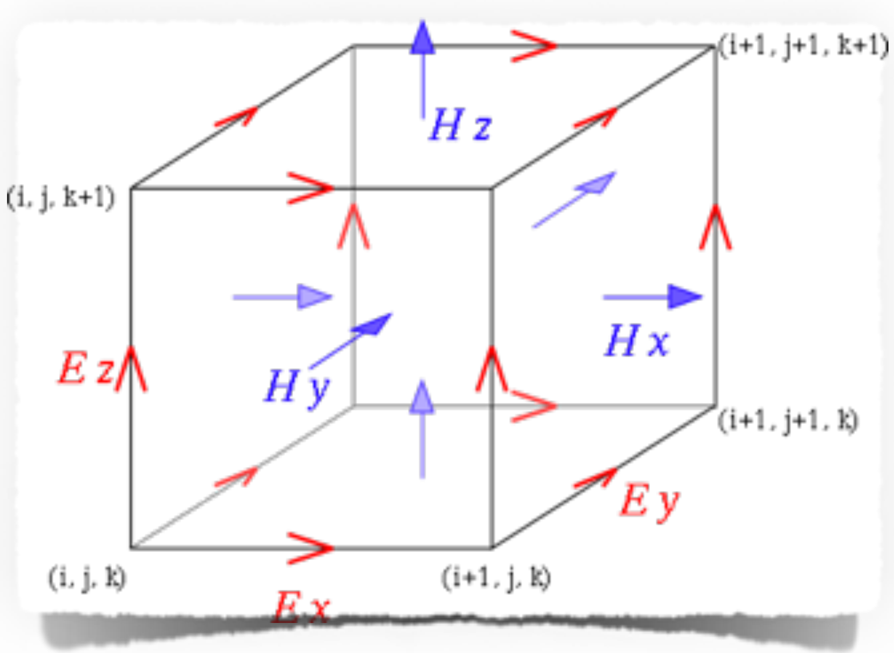

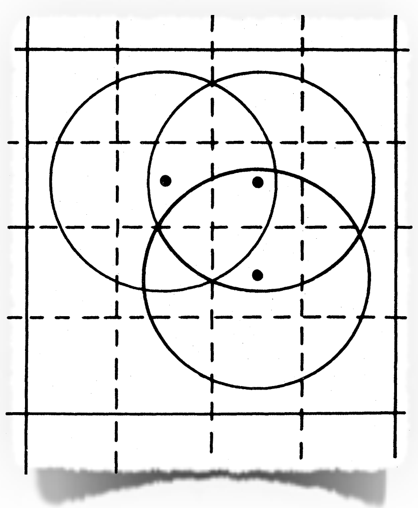

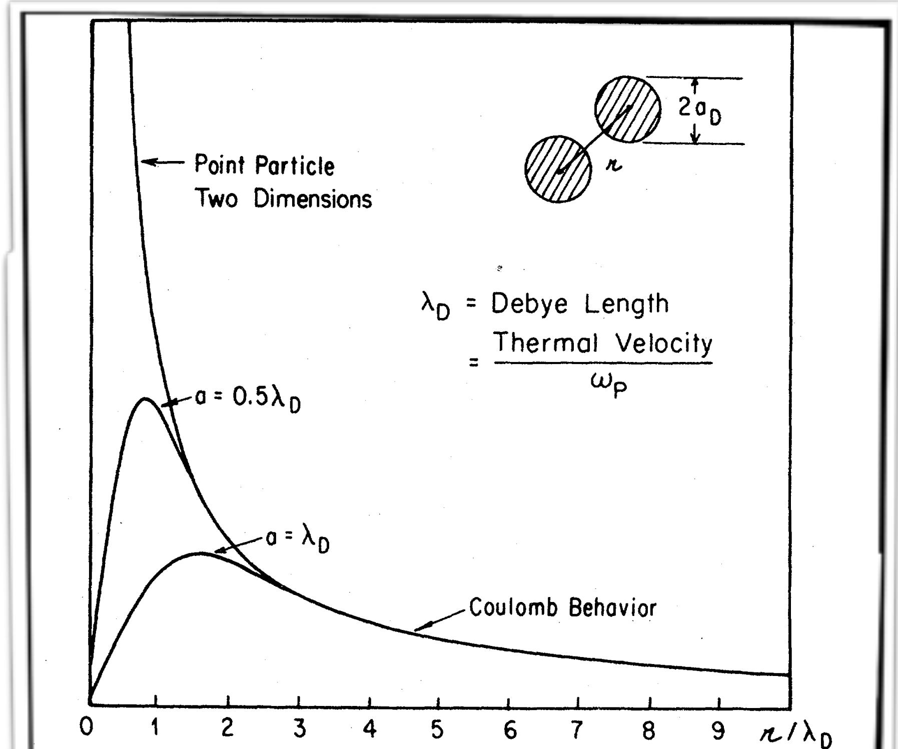

FIG. 2. Force law between finite-size particles in two dimensions for various sized particles. A Gaussian-shaped charge-density profile was used.

Dawson '83

Nonlinear perpendicular high M_A shock structure

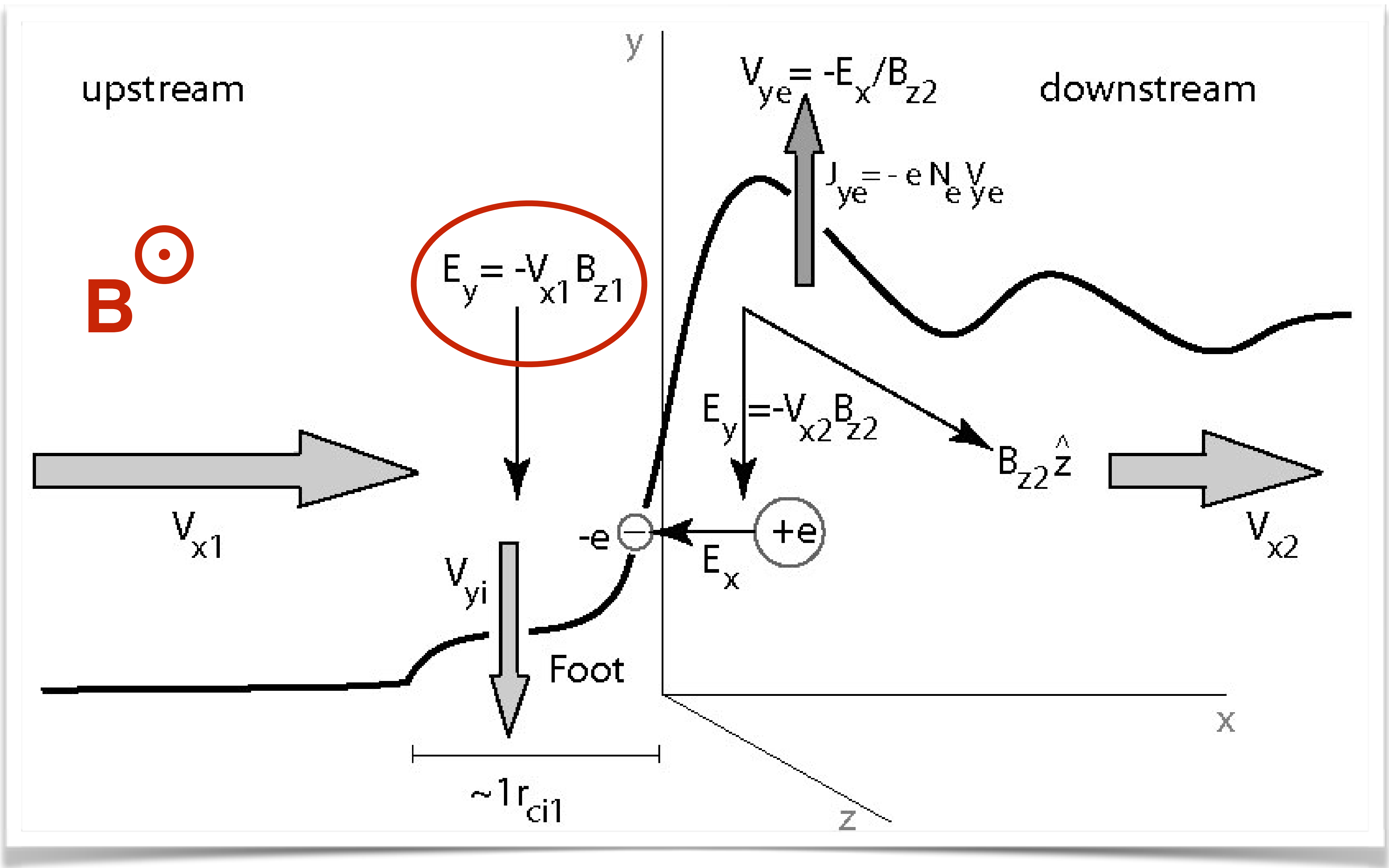

Treumann & Jaroschek (2008)

- portion of incoming ions reflected from the shock-potential electric field
- reflected ions accelerated in the upstream convection electric field (grad-B drift)

Structure of a high M_A shock

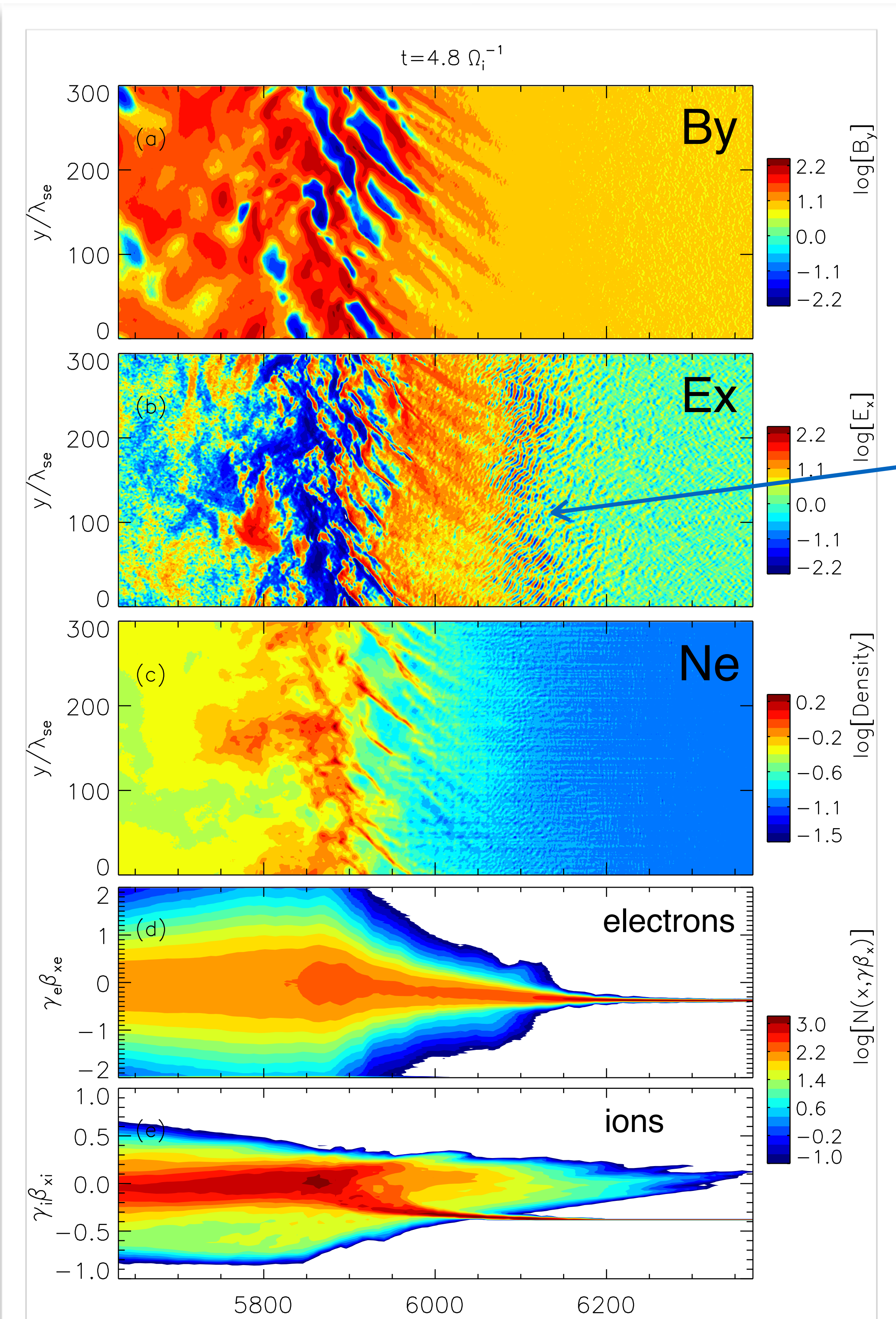

Forward shock at t=4.8 Ω_i^{-1}

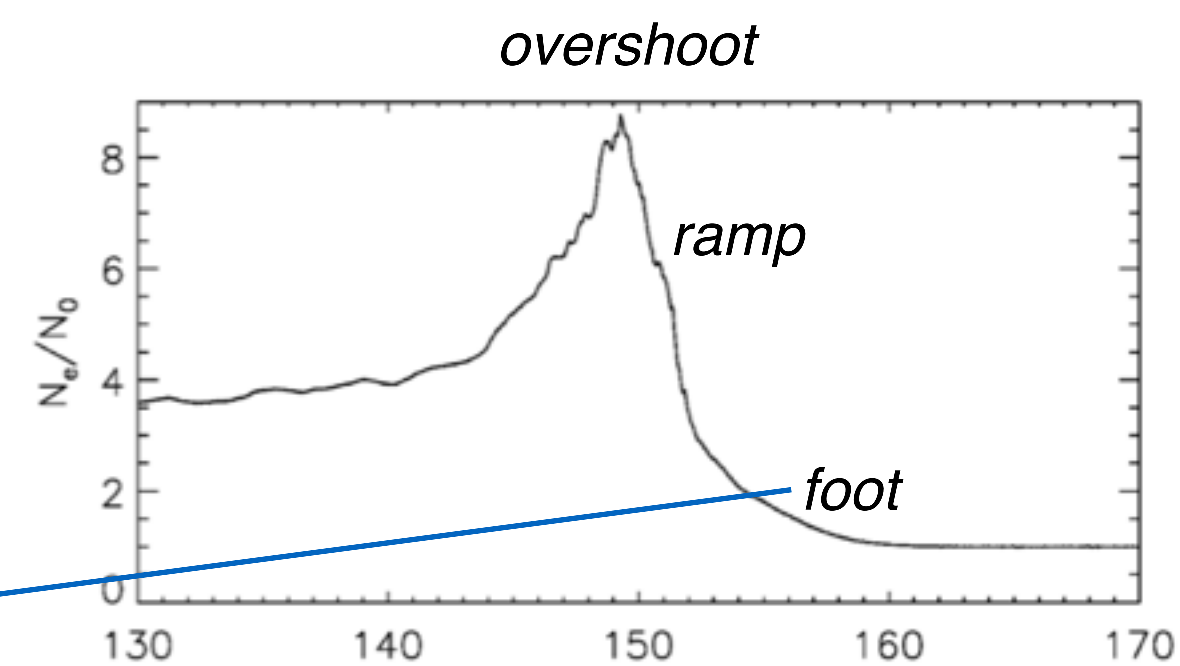

- structure governed by ion reflection
- gyrating reflected ions excite ion beam Weibel-type instability that generates magnetic filaments in the shock ramp
- interaction between reflected ions and incoming electrons leads to electrostatic Buneman instability in the shock foot

PIC simulations:

Wieland et al. (2016); M_A=28

Shock reformation…

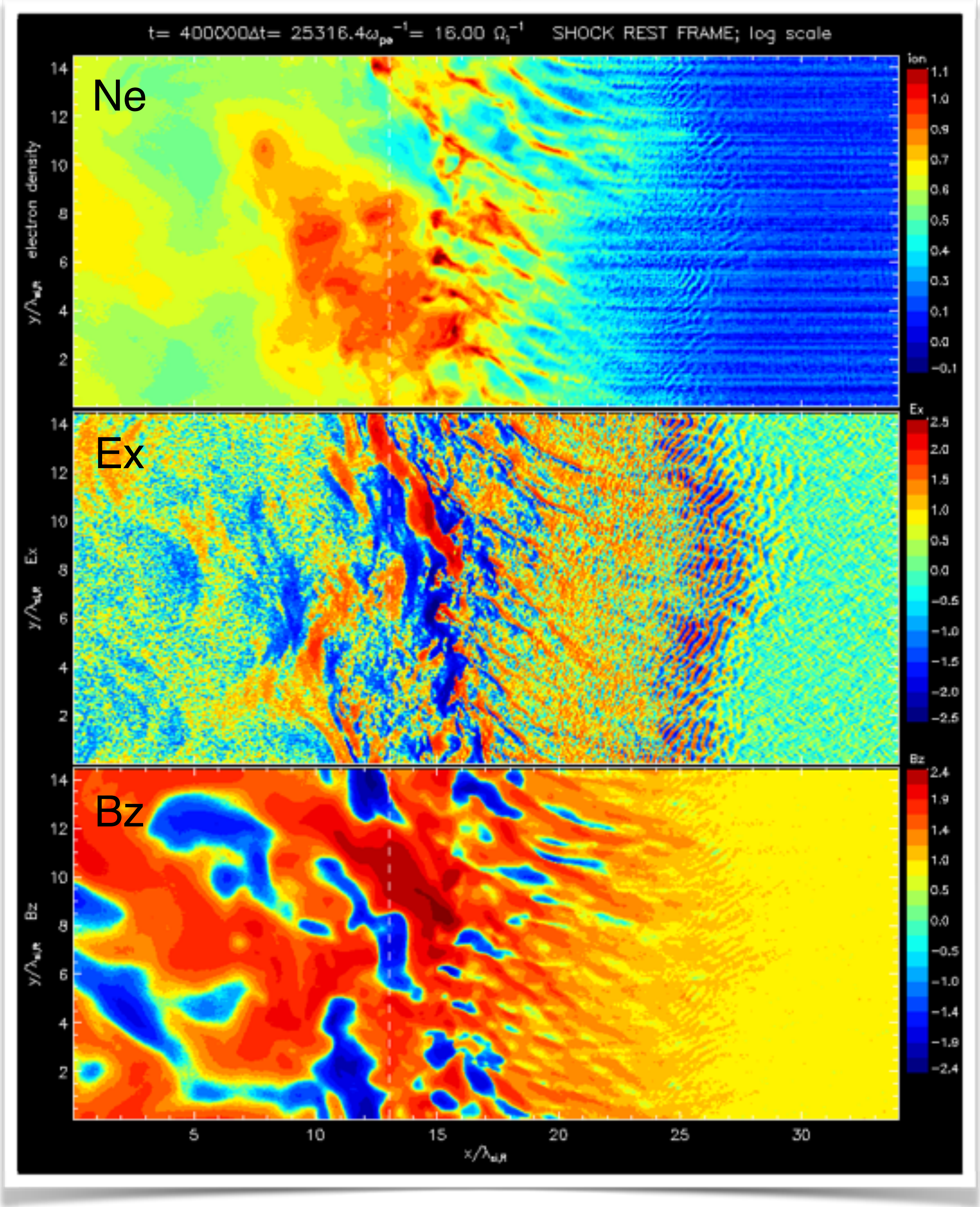

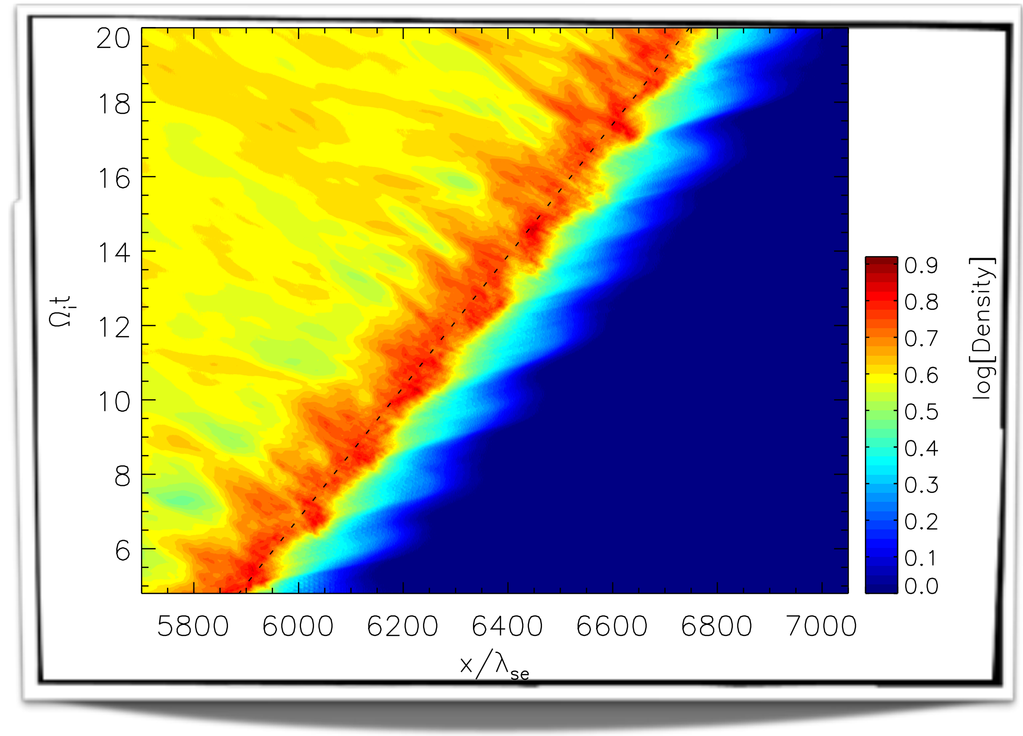

- cyclic shock self-reformation caused by non-steady dynamics of ion reflection from the shock and governed by the physics of current filament mergers in the shock ramp
- period of ~1.5 Ω_i^{-1}
- electron injection efficiency time-dependent

shock rest frame

Shock reformation… and rippling

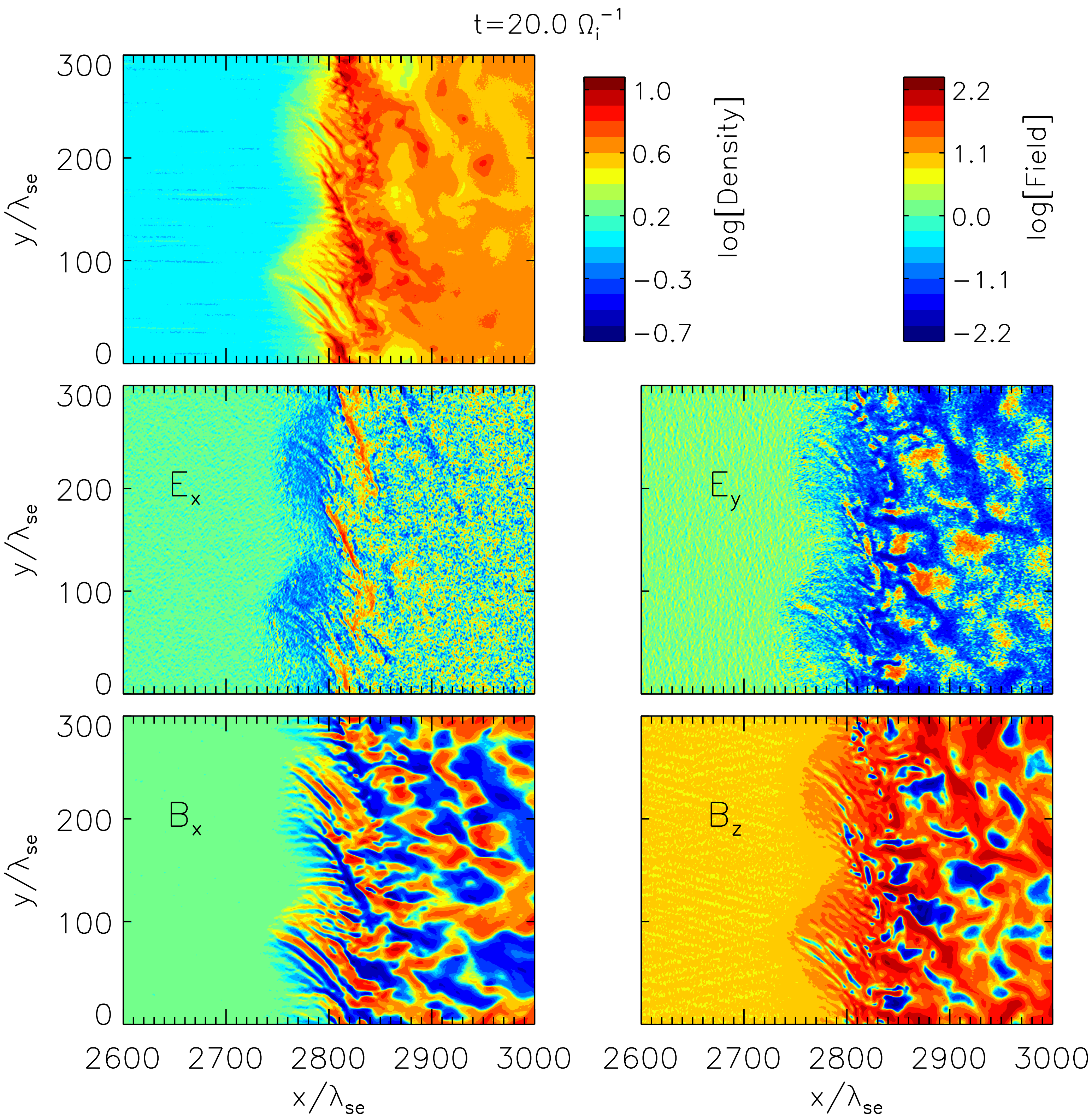

- spatial (~20 λ_{si}) and temporal scales given by gyro-motion of the shock-reflected ions spatially modulated along the shock surface (Burgess & Scholer (2007) for low-Mach-number shocks)
- enhanced localized electron heating and acceleration should occur
- rippling on scales of a few λ_{si}, driven by ion temperature anisotropy (AIC) in the shock ramp not observed

Electron injection

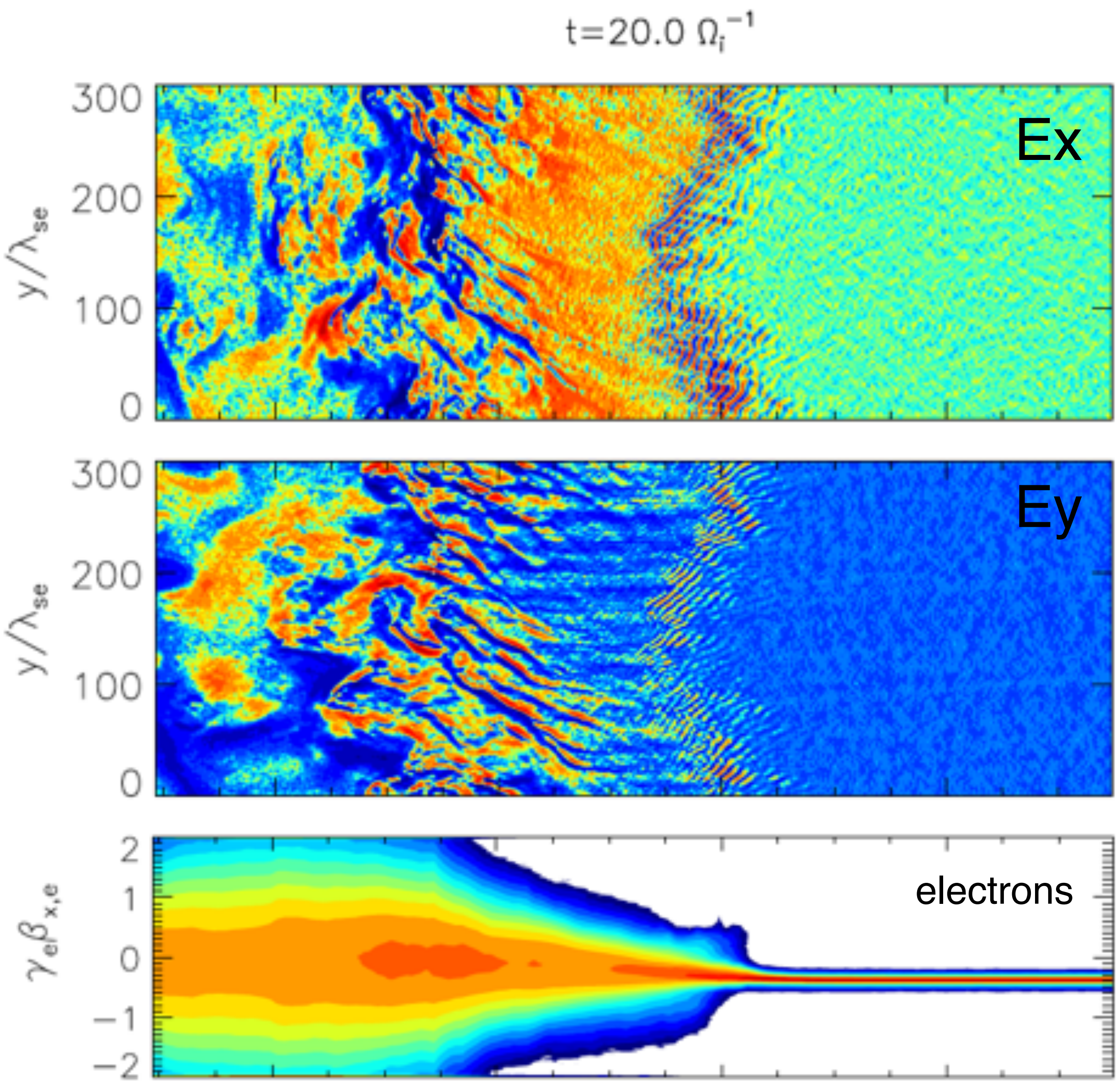

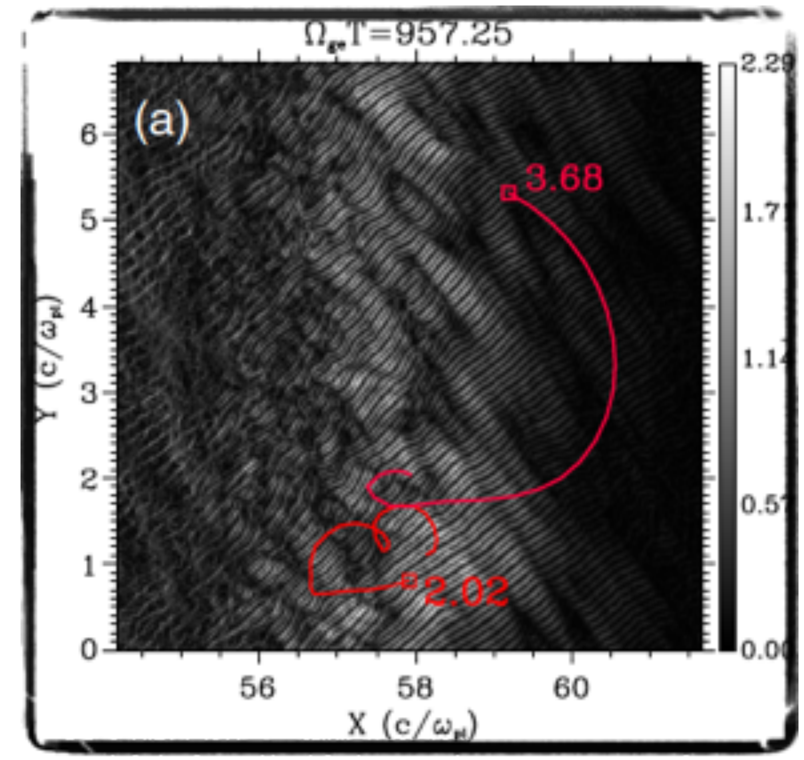

Matsumoto et al. 2013

- electron shock-surfing acceleration (SSA)
  - stochastic acceleration of particles trapped in strongly nonlinear electrostatic Buneman waves
  - electrons escaping upstream further accelerated in the motional electric field
- both instability and trapping conditions need to be met
- acceleration efficiency strongly depends on dimensionality effects

instability for $\Delta V > v_{the}$ $$M_A \geqslant \frac{1+\alpha}{2}\sqrt{\beta_e}\left(\frac{M}{m}\right)^{\frac{1}{2}}$$

trapping for $E_B \gg cB_0$ $$M_A \geqslant (1+\alpha)\left(\frac{M}{m}\right)^{\frac{2}{3}}$$

2D PIC simulations of perpendicular shocks

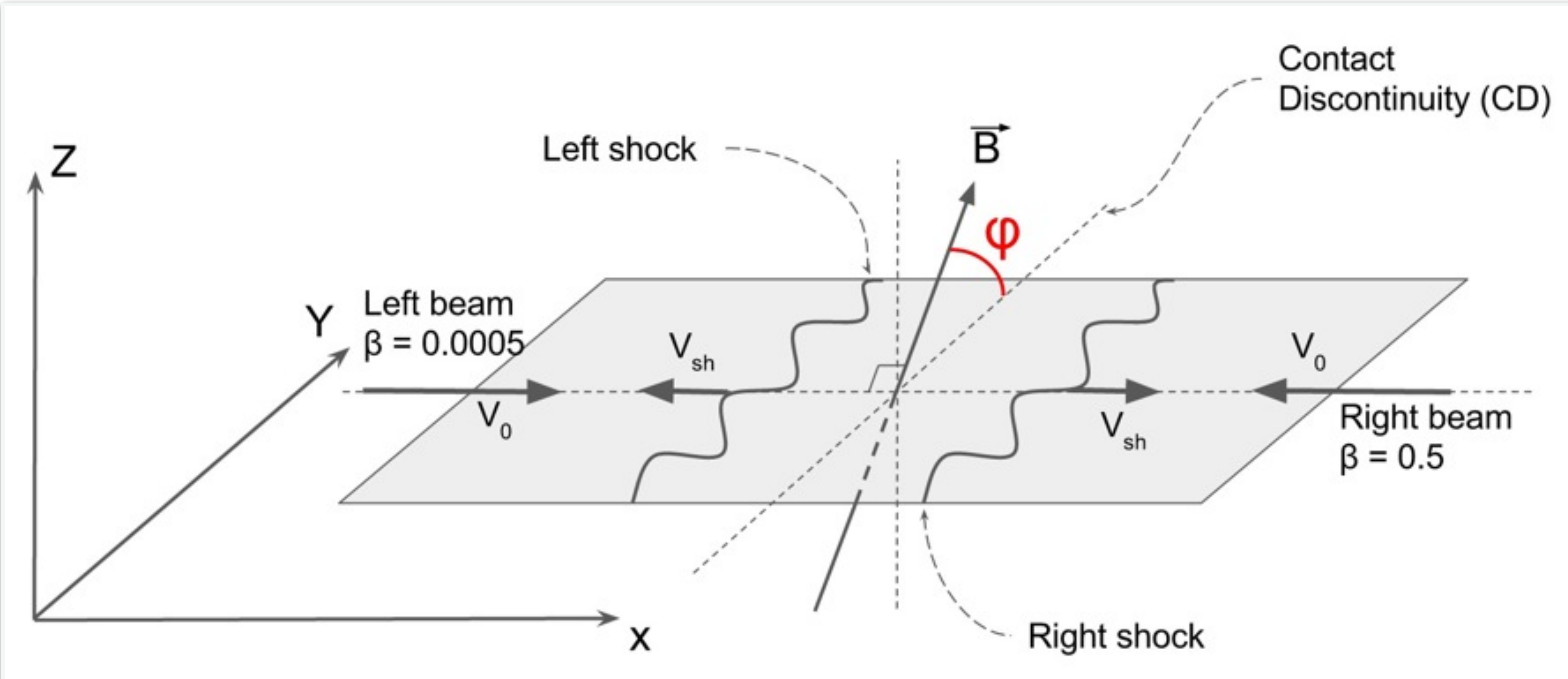

Simulations with different magnetic field geometry:

φ = 0° - in-plane

φ = 45°

φ = 90° - out-of-plane

M_A=32, M_s=1550 (50)

Bohdan et al. (2017)

Electron injection at a perpendicular shock in two dimensions:

effects of the choice of a 2D simulation plane

- work building up on results by Hoshino & Shimada (2002), Amano & Hoshino (2009 a,b), Matsumoto, Amano & Hoshino (2012, 2013), Matsumoto et al. (2015), Wieland et al. (2016), ++

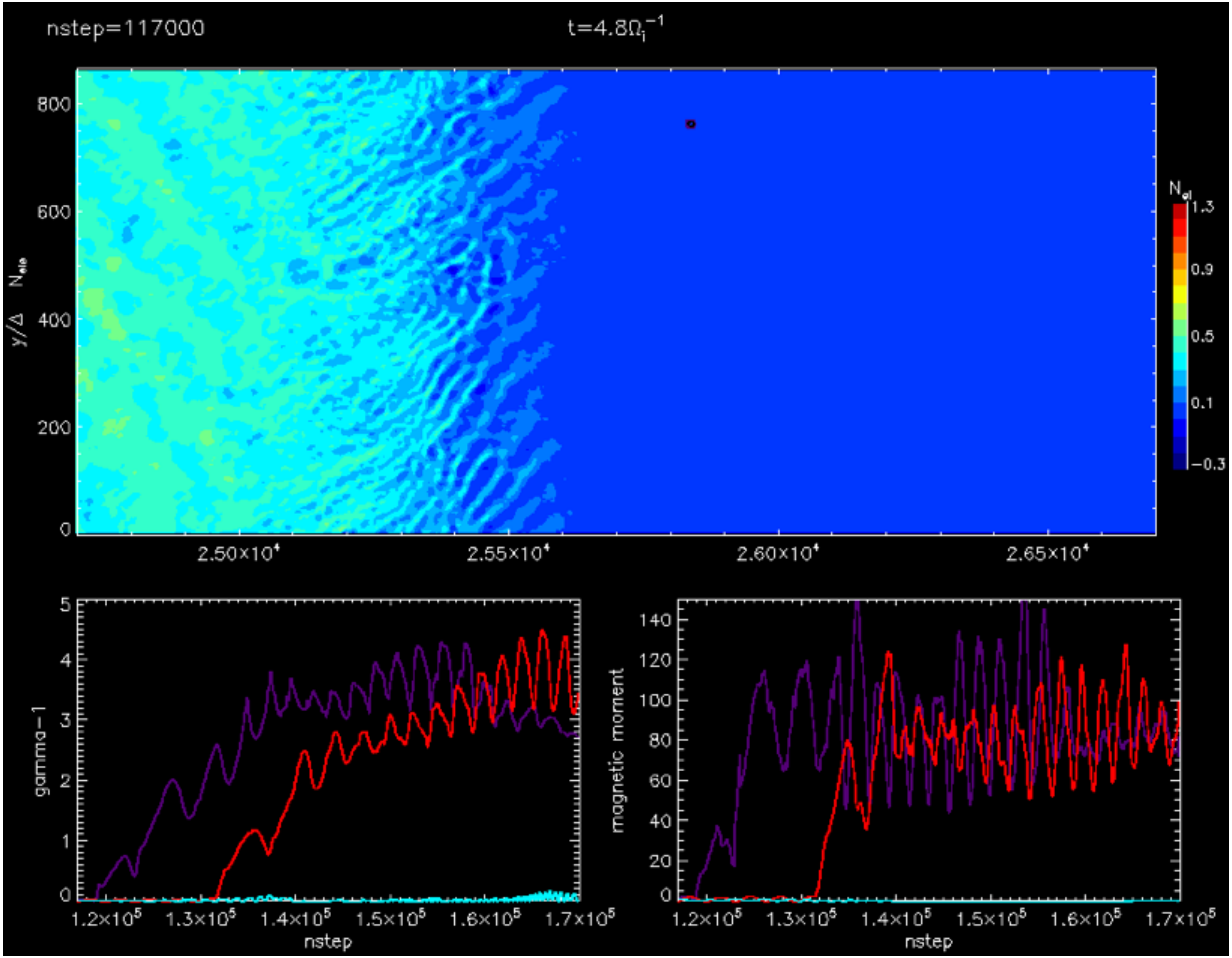

φ=90°
out-of-plane

- double interaction with Buneman waves (red and violet particles) followed by adiabatic acceleration in the shock ramp through grad-B drift

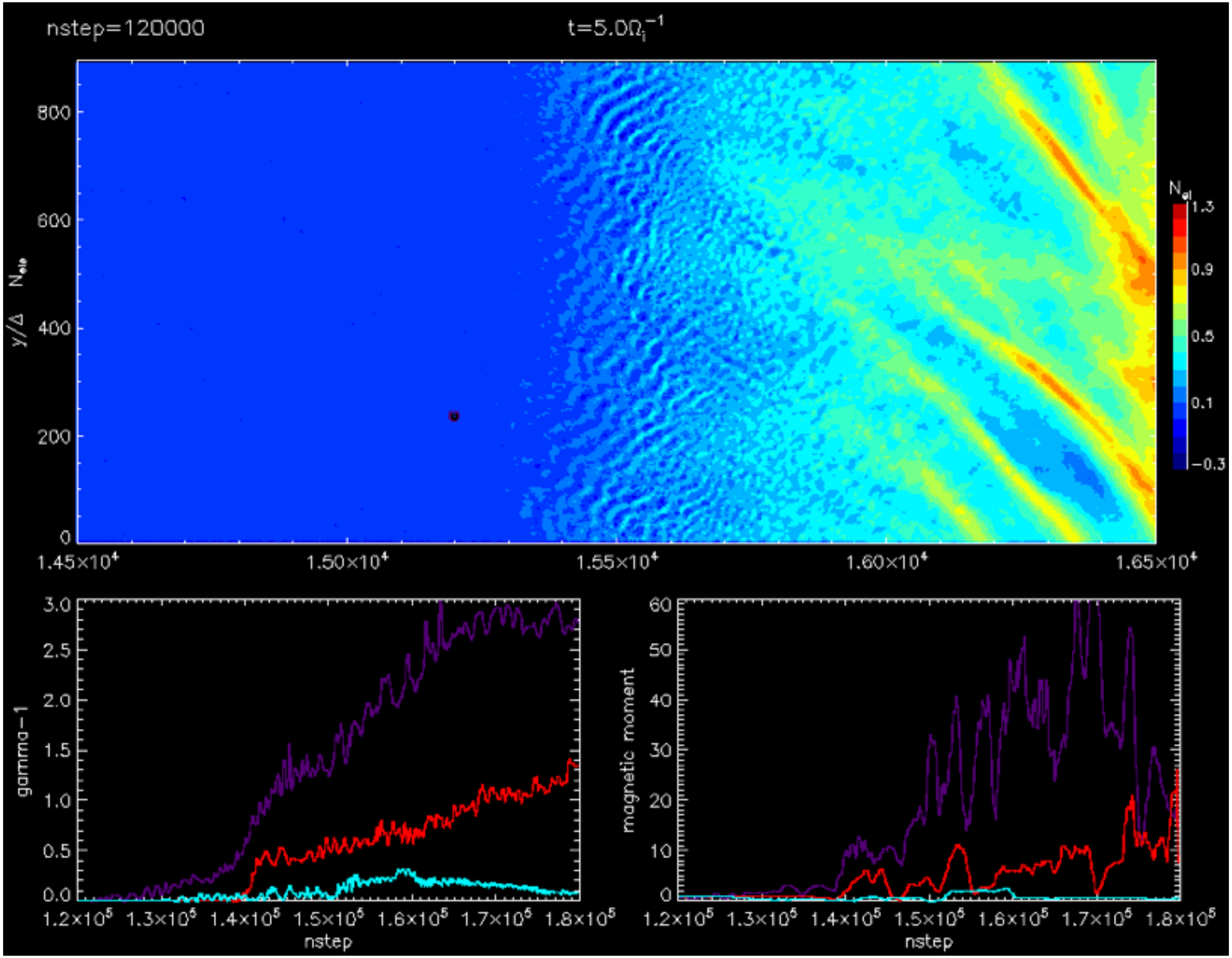

φ=45°
(and φ=0°)

- interaction with Buneman waves (red and violet particles) followed by non-adiabatic acceleration in collissions with moving magnetic structures

Spontaneous turbulent reconnection

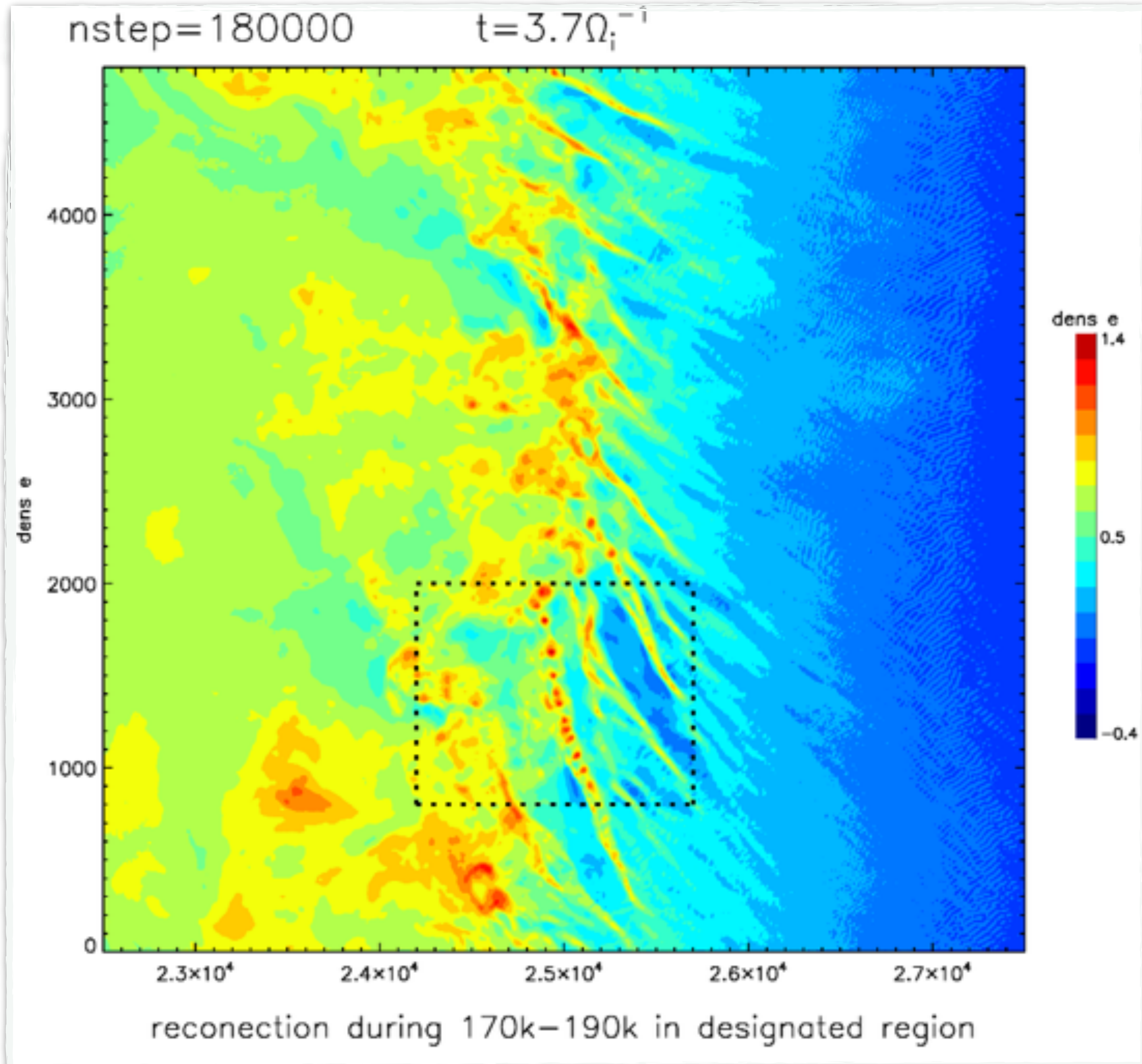

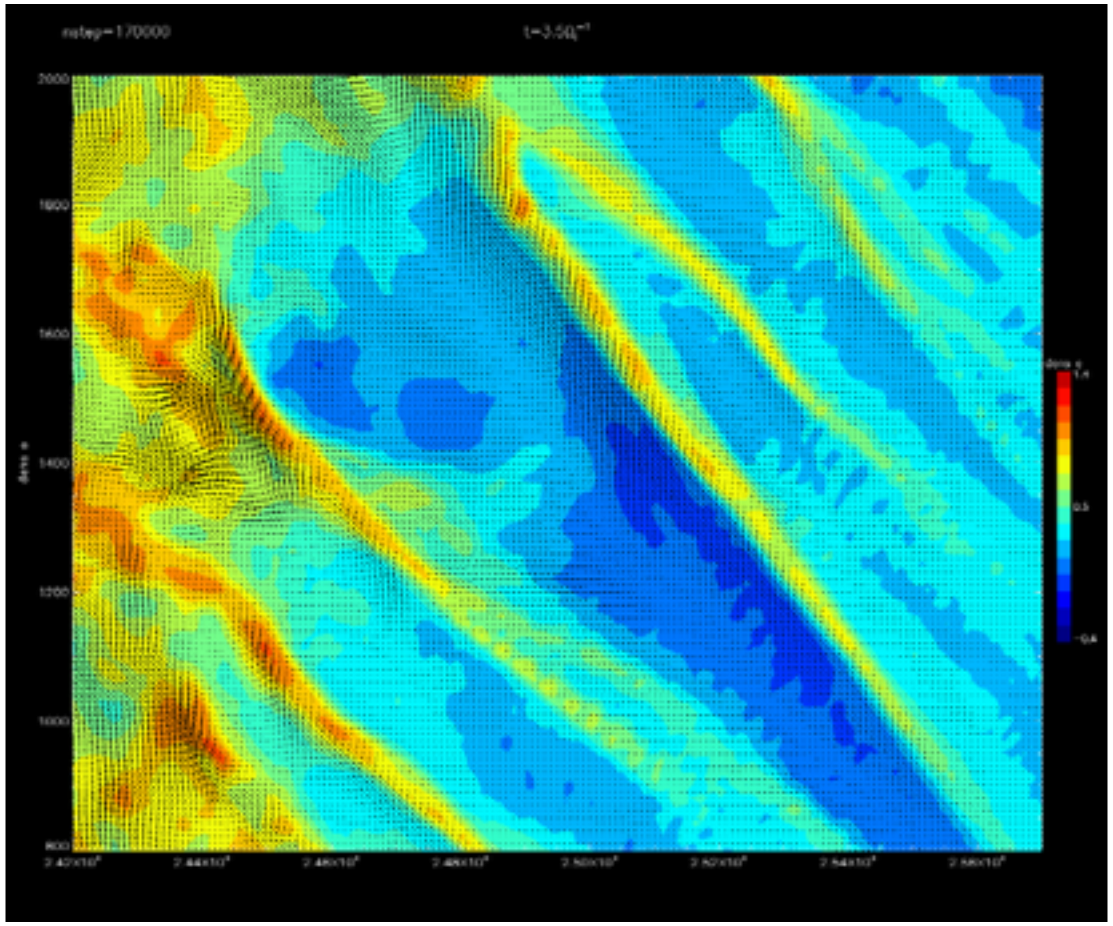

$\vartheta = 45^o$

$\sim 0.4\Omega^{-1}$

- magnetic reconnection takes place in current sheets within filamentary shock transition and downstream. As a result, magnetic islands are formed along current sheets.
- turbulent reconnection observed only for in-plane (0^o) and oblique (45^o) configurations
- the process is intermittent, effectiveness vary with the phase of cyclic shock reformation
- additional electron energization occurs (Matsumoto et al. 2015) - **see talk by A. Bohdan**

Electron acceleration efficiency

- acceleration most efficient for out-of-plane magnetic field configurations

- spectra vary with the phase of the cyclic shock reformation and plasma beta β_p (temperature)

- maximum efficiency (nonthermal electron fraction) in moderate-temperature plasmas (β_p=0.5) varies from ~0.5% for φ = 0° and 45° and ~7% for φ = 90°

- in cold plasmas ($\beta_p \ll 1$) acceleration efficiencies a factor of 2-3 smaller

Downstream electron spectra normalized to dowstream temperature:

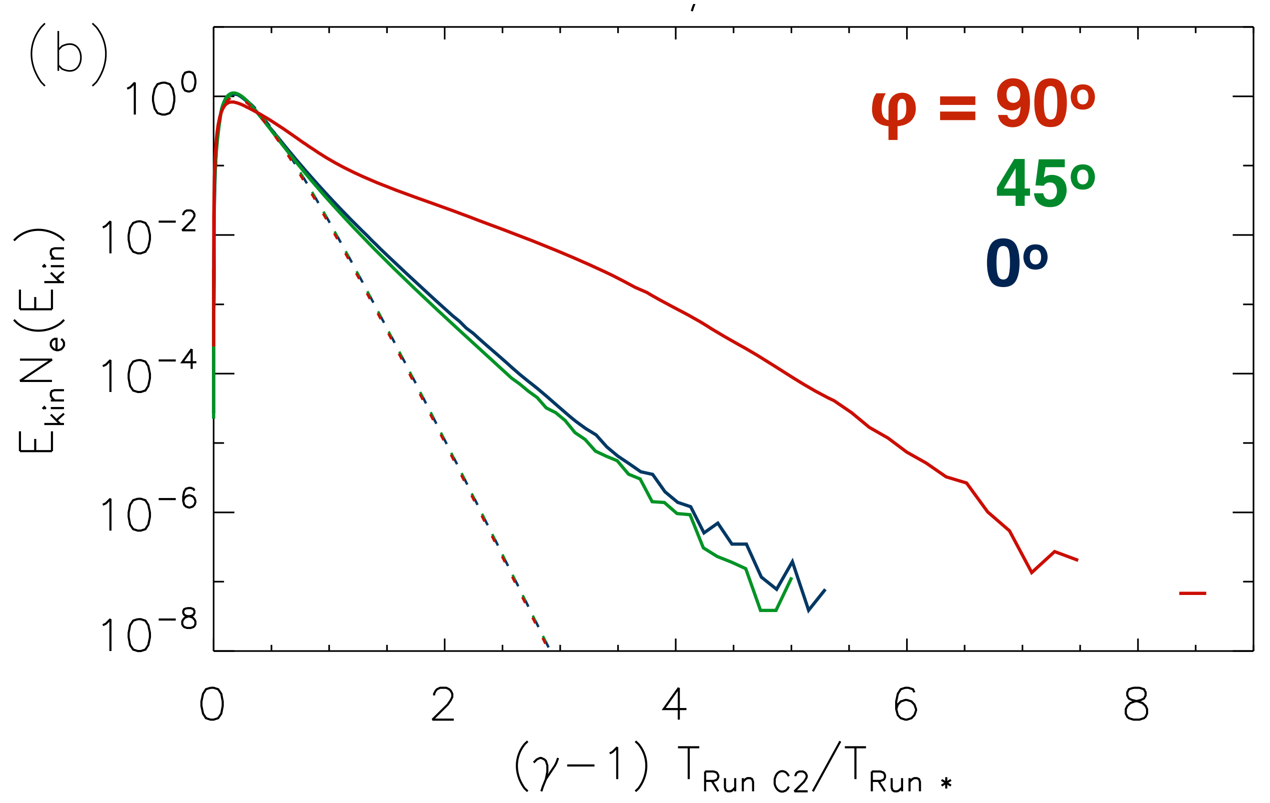

Buneman wave structure

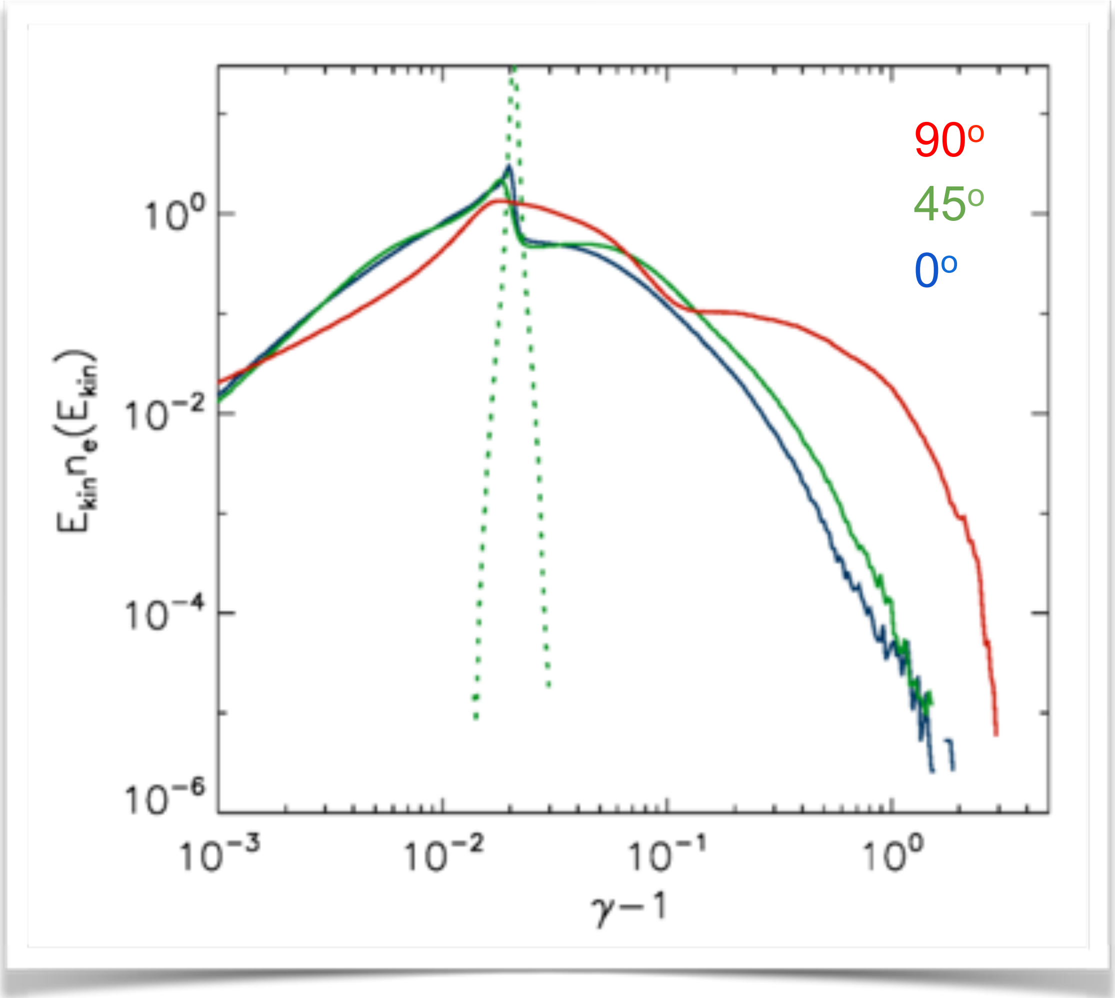

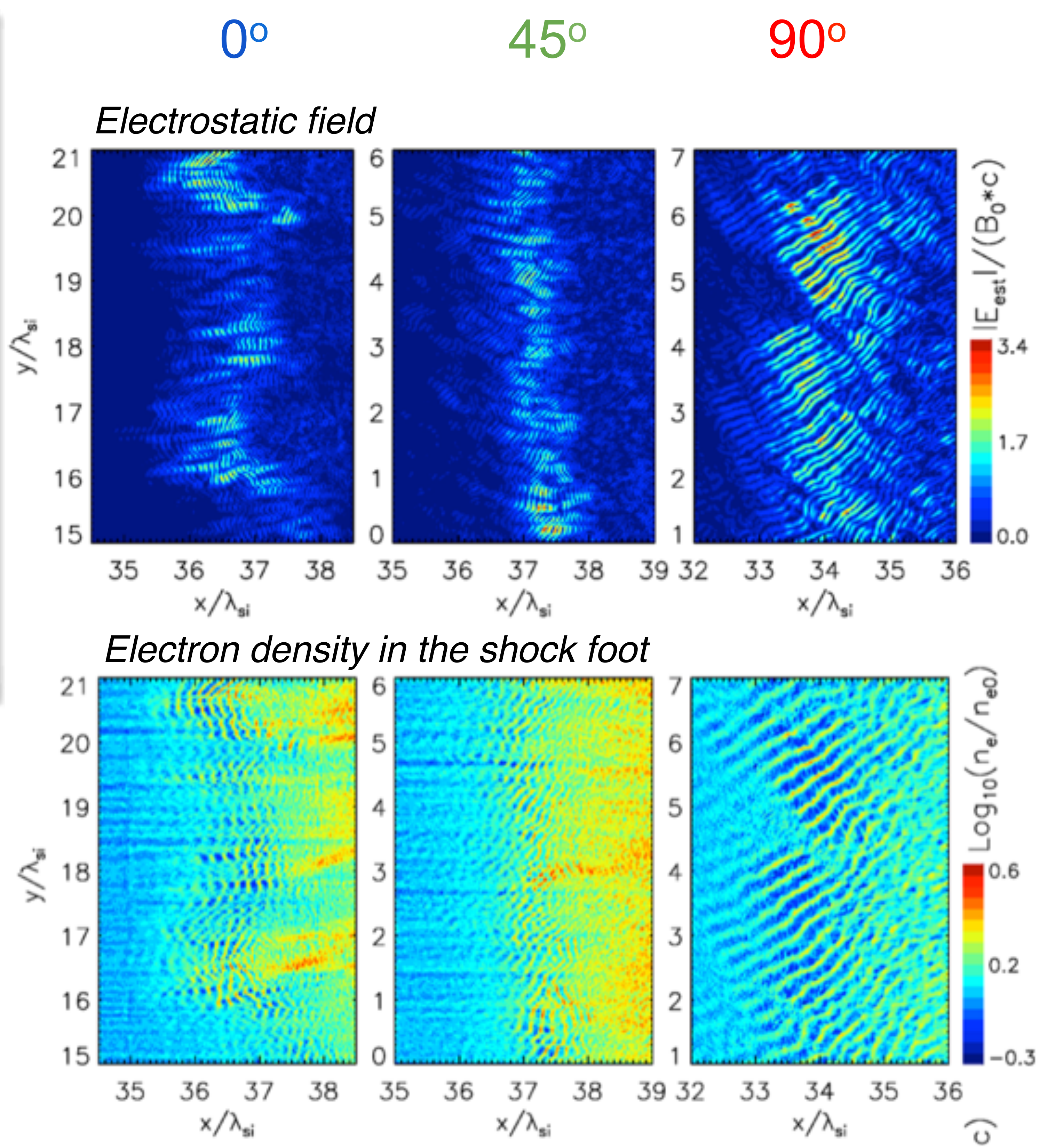

- fraction of nonthermal particles largely determined in the shock foot – wave intensity and structure of the Buneman wave zone is a major factor

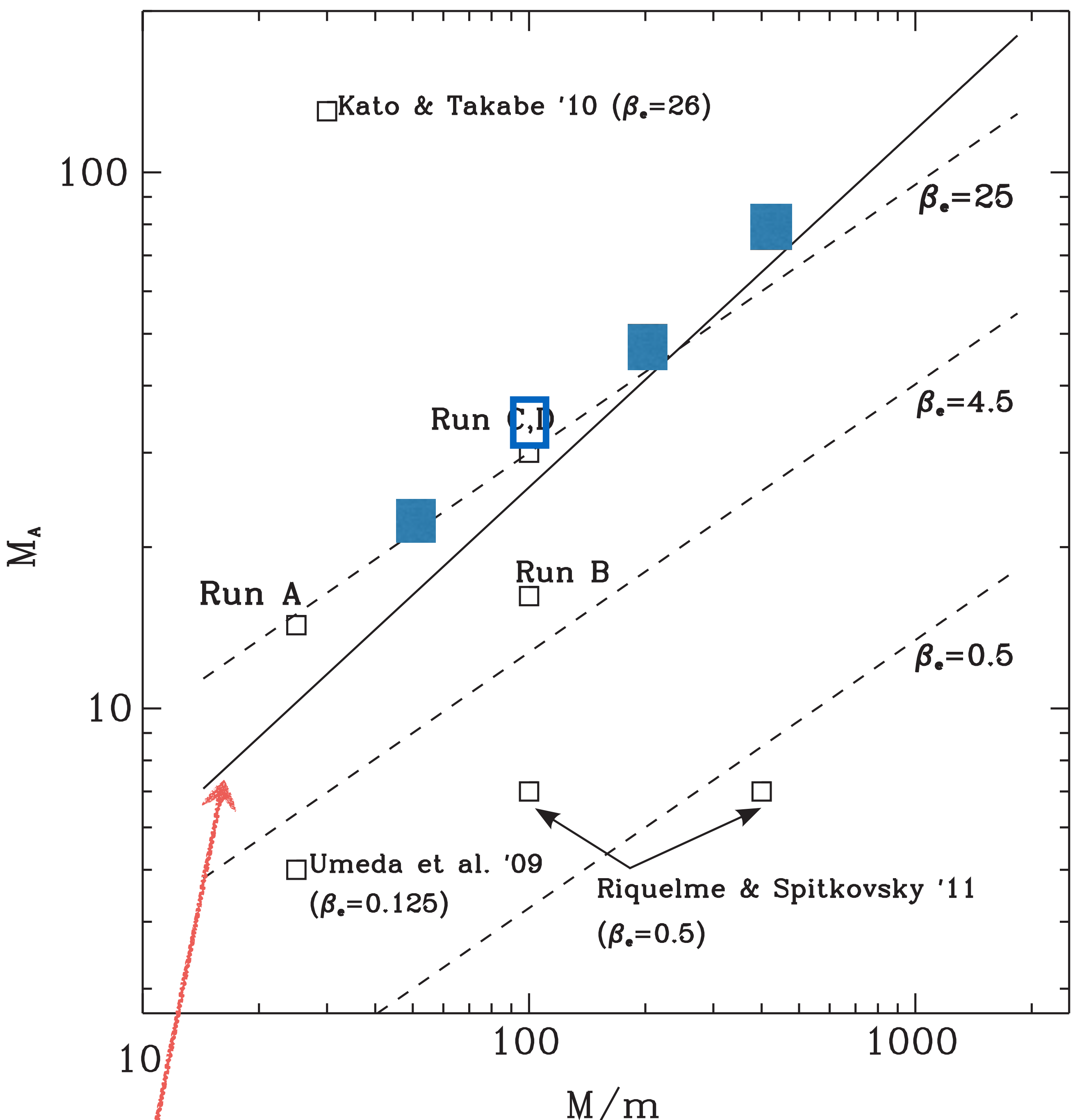

$$M_A \geqslant (1+\alpha)\left(\frac{M}{m}\right)^{\frac{2}{3}}$$

trapping condition
(linear theory, cold plasma, out-of-plane mf

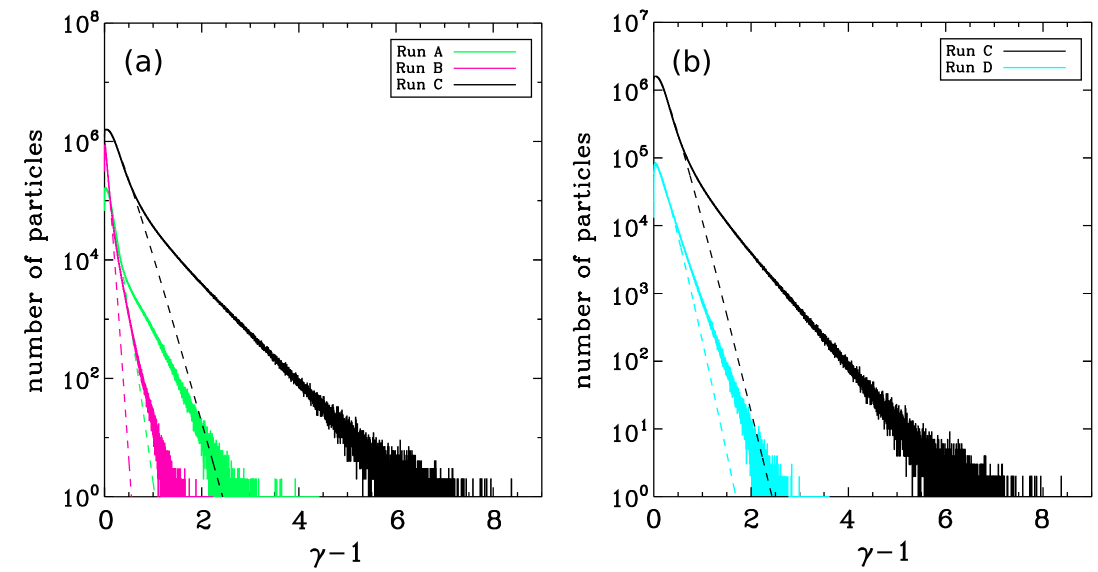

	M_A	M/m	β_e	ω_{pe}/Ω_{ge}	Equation (5)	Equation (8)	Ele. Accel.
Run A	14.4	25	0.5	10	2.1	10.3	BI
Run B	16.2	100	0.5	10	4.2	25.8	Weak
Run C	30.0	100	0.5	10	4.2	25.8	BI + adiabatic
Run D	30.0	100	4.5	10	12.7	25.8	Weak

■ simulations by Bohdan et al. (2017a,b)

- SSA inefficient in high β plasmas - linear theories of the Buneman instability in cold plasmas do not apply

Electron injection in three dimensions

3D PIC simulation of a quasi-perpendicular subluminal shock

Matsumoto et al. (2017)

3D3V, M_A=20.8, M_s=22.8, ϑ=74.3°, m_i/m_e=64, β=1

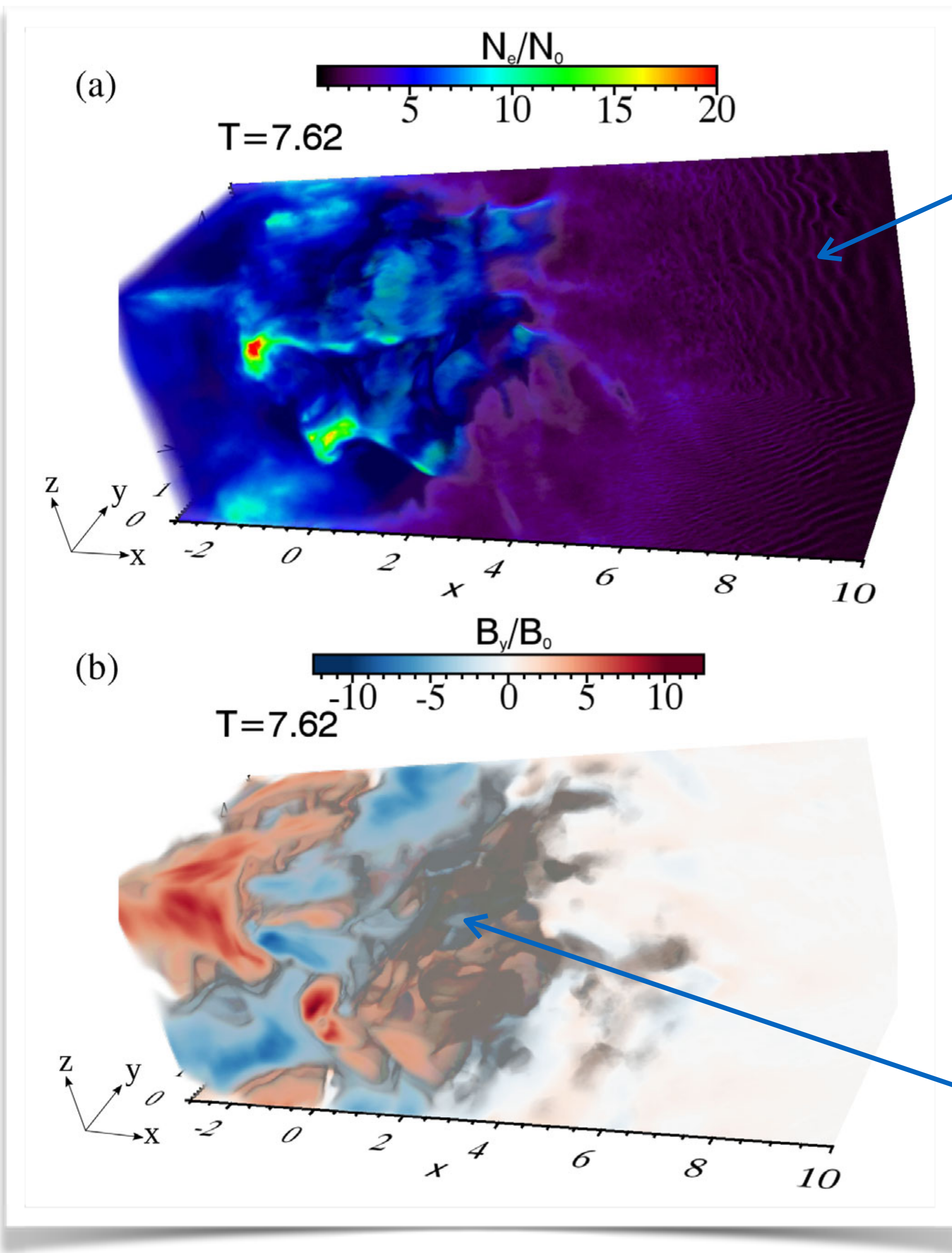

coherent electrostatic structures in the shock foot ($|E|>B_0$)

- Buneman and Wiebel instabilities coexist in different regions of the shock transition

strong ion-Weibel turbulence in the shock ramp

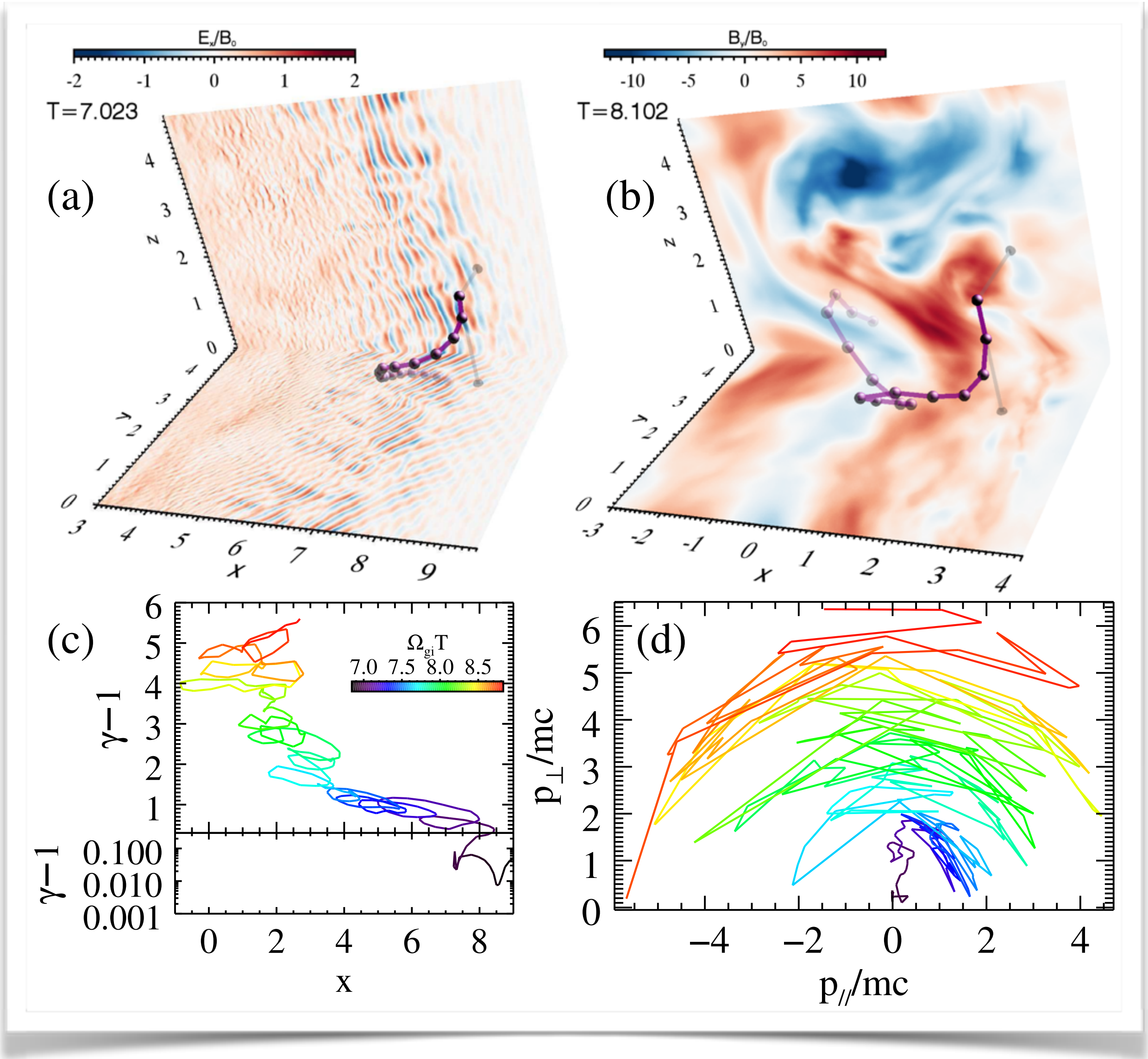

Sample energetic particle

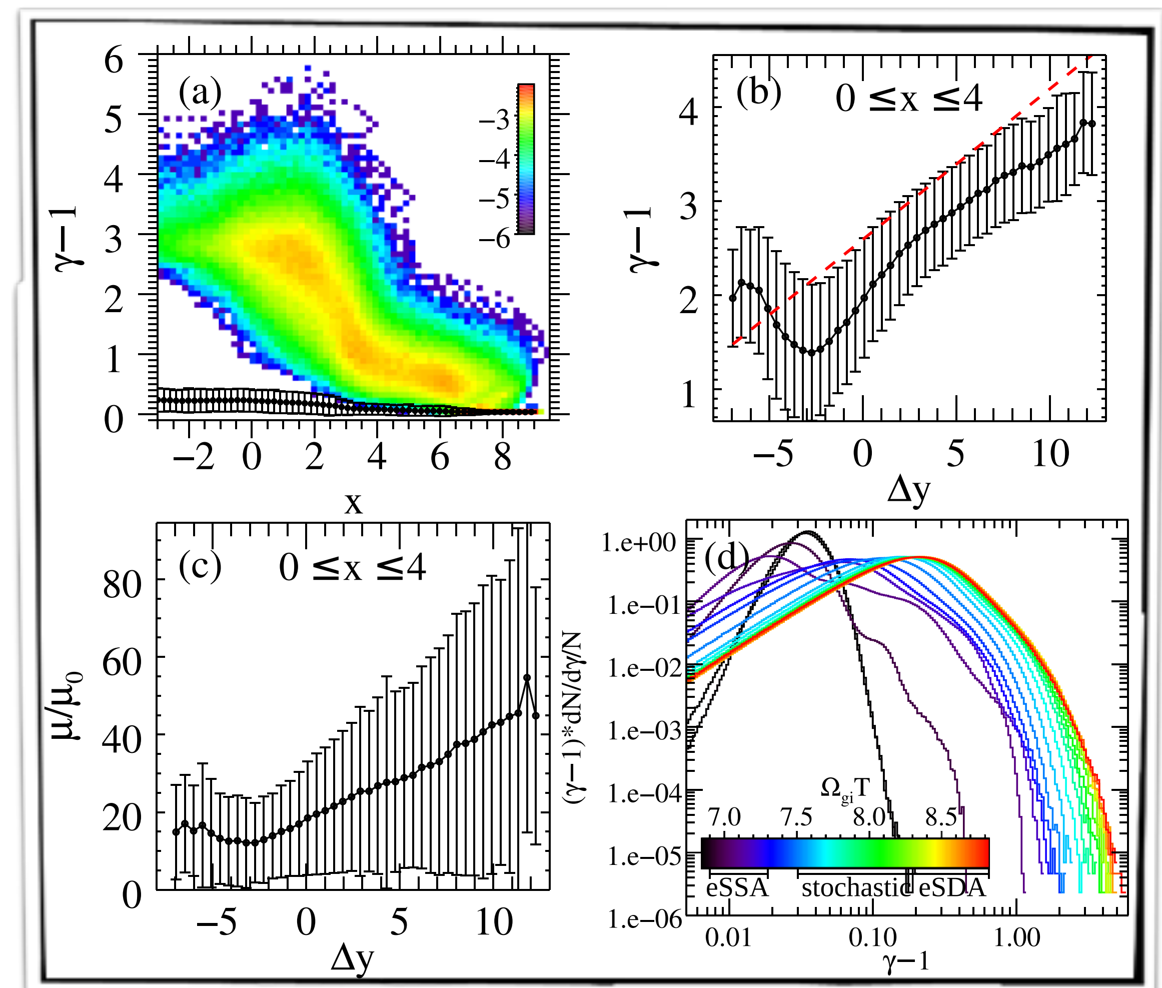

Ensamble of energetic particles

- first-stage acceleration via SSA
- subsequent continuous acceleration through pitch-angle scattering by magnetic turbulence
- average energy gain through drift in motional electric field (as in SDA) but process is nonadiabatic - stochastic SDA
- supra-thermal tails evolves with time to higher energies

2D vs 3D

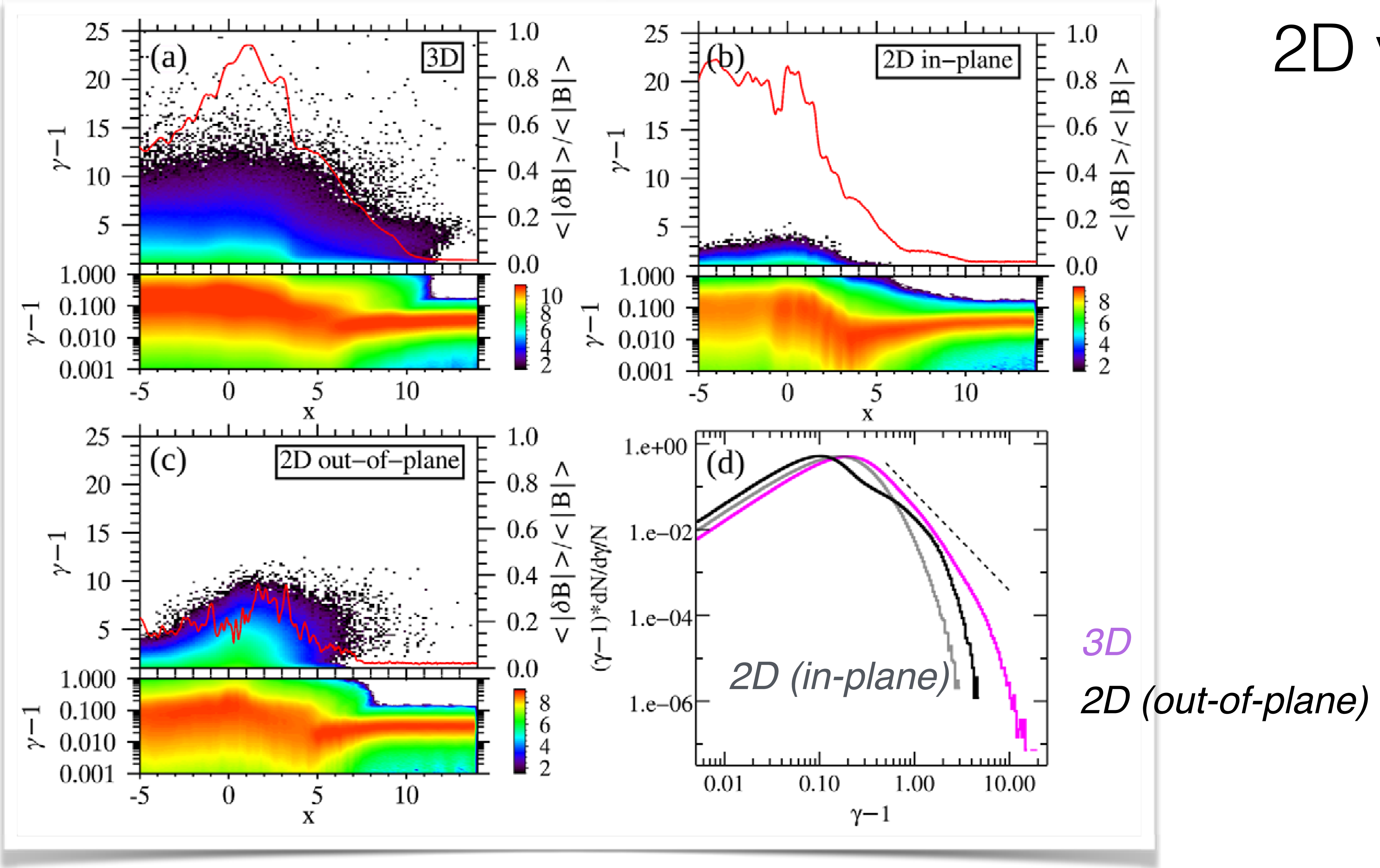

- systems lacking either SSA or Weibel turbulence cannot provide efficient supra-thermal particle production
- magnetic reconnection in the Weibel turbulence not observed - too small MA (mass ratio)
- following acceleration through scattering on self-generated waves excited upstream by accelerated electrons?

Critical Mach number for electron injection

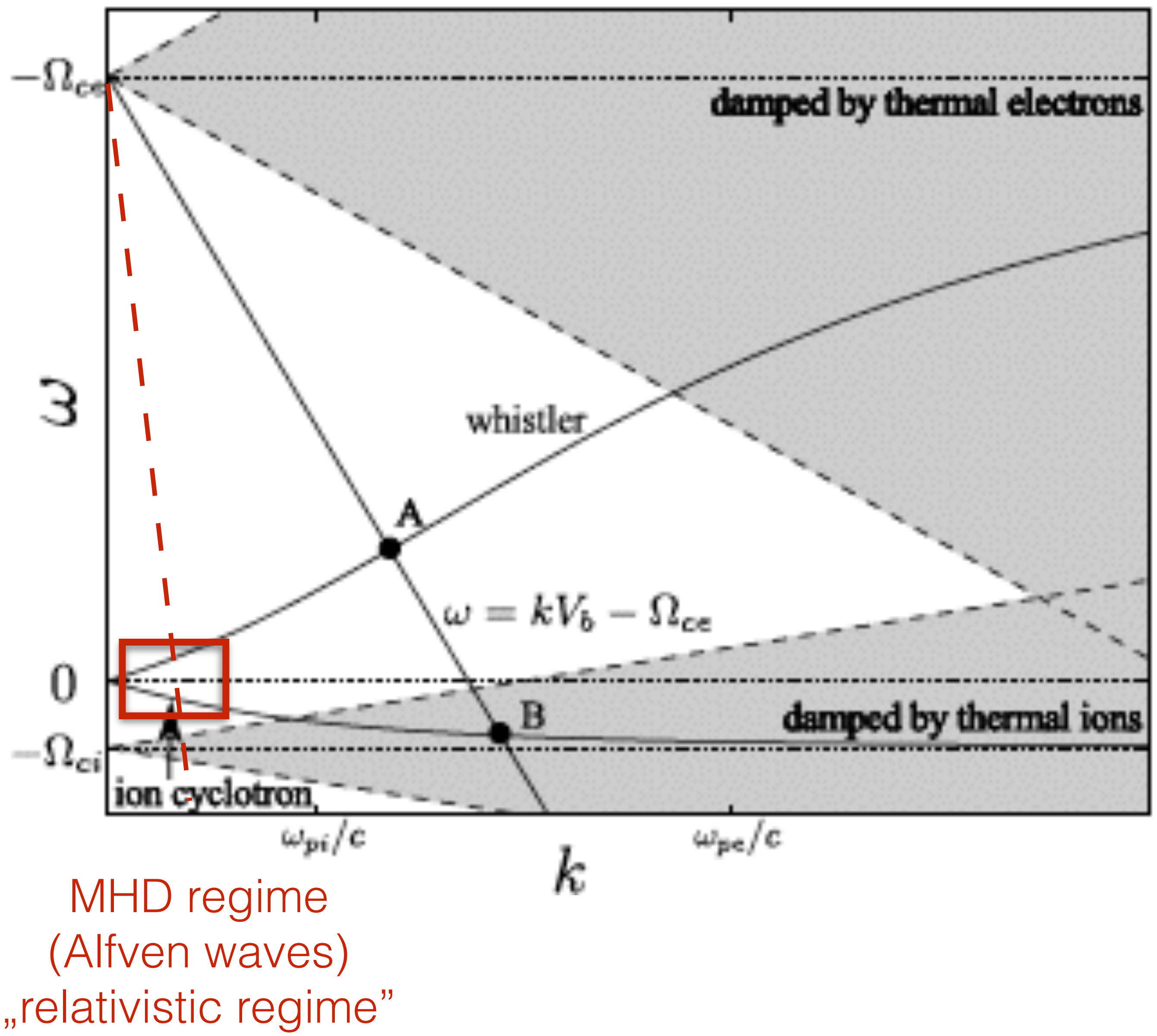

- electron scattering under resonant condition requires high-frequency whistler waves

$$\omega - kv_{\|} = \Omega_c/\gamma$$

- interaction of a cold electron plasma beam with whistler waves (A) prohibited by the momentum conservation law
- interaction of truly nonrelativistic beam with ion cyclotron wave (B) need to overcome damping by thermal ions
- all simulation work so far performed for „relativistic" beams that probe MHD regime

Critical Mach number for electron injection

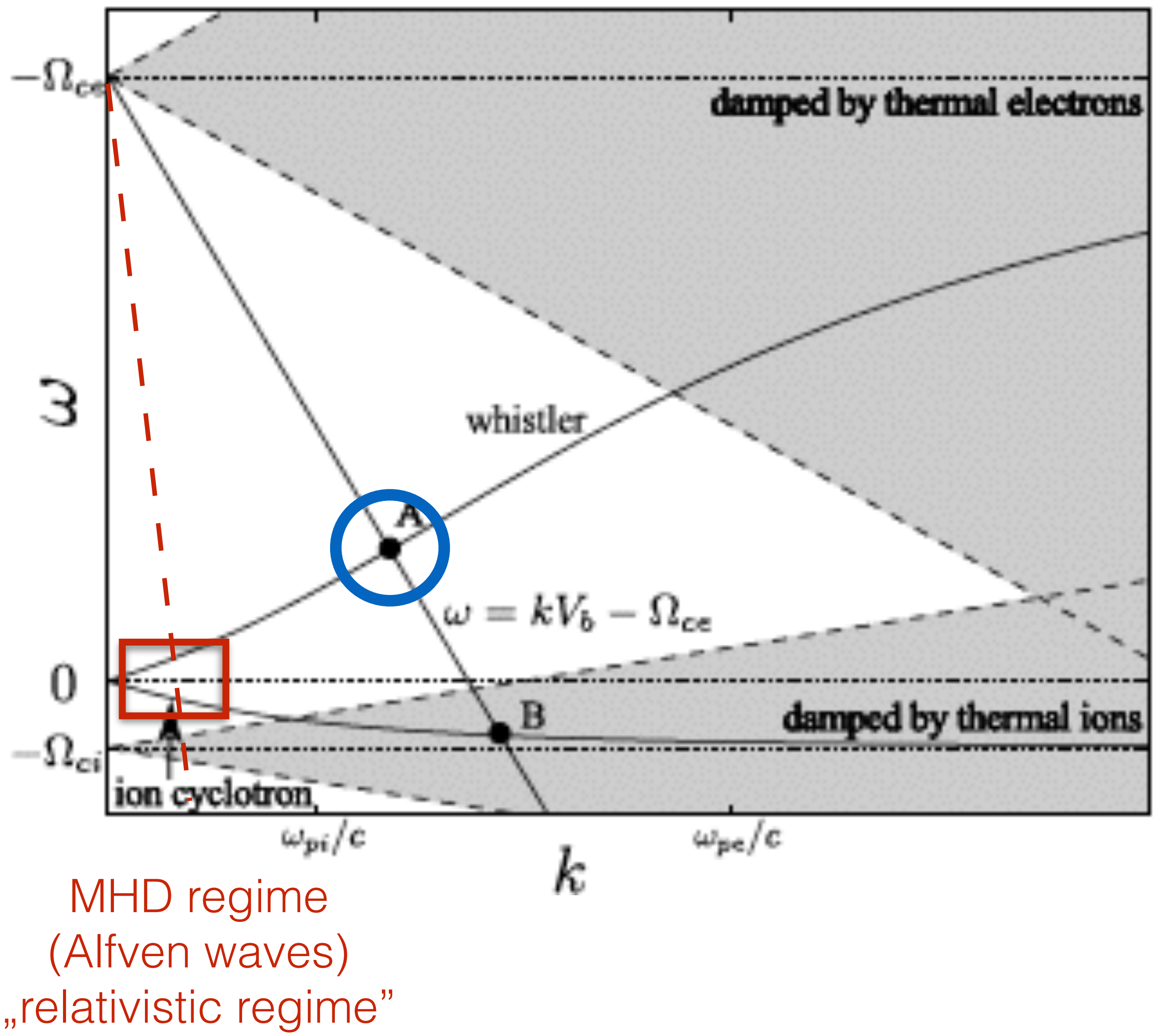

- whistler wave (A) can be destabilized in a presence of the loss-cone distribution (natural consequence of mirror reflection - SDA)
- critical Mach number for injection:

$$M_A \gtrsim \frac{\cos\theta_{Bn}}{2}\sqrt{\frac{m_i}{m_e}\beta_e} \equiv M_A^{\mathrm{inj}}.$$

Amano & Hoshino 2010

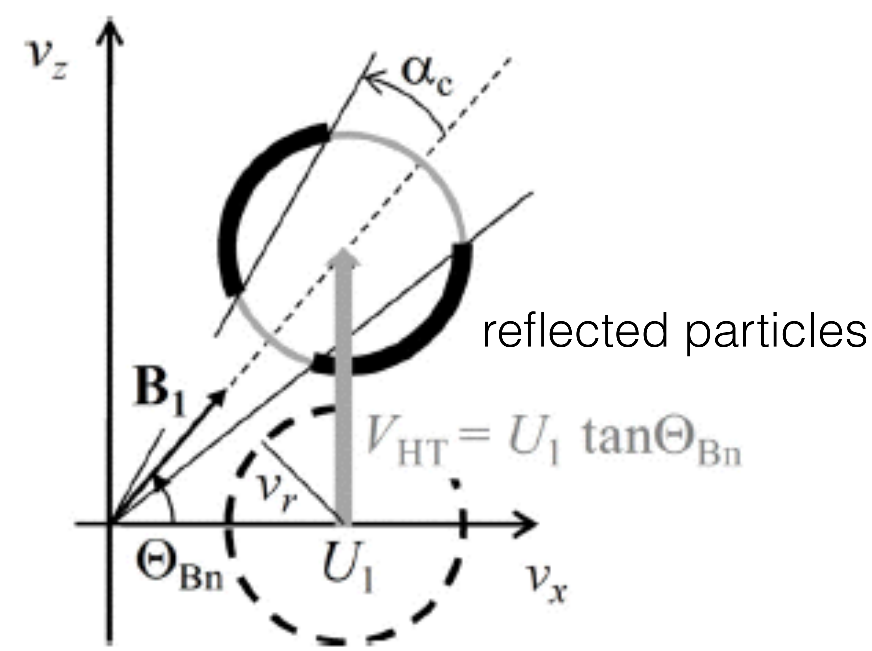

Critical Mach number for electron injection

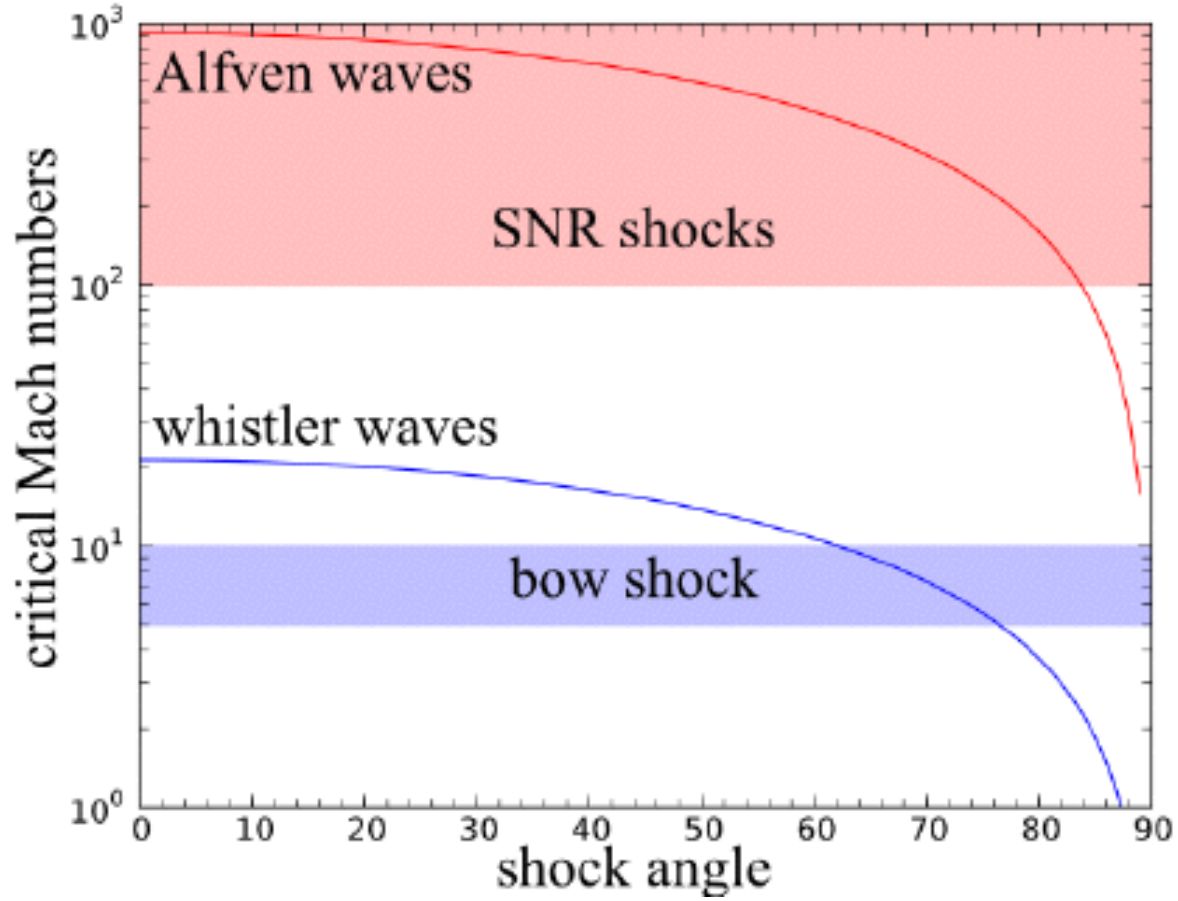

- mechanism naturally explains injection in SNRs
- can be tested via in-situ observations (e.g., at Earth's bow shock)

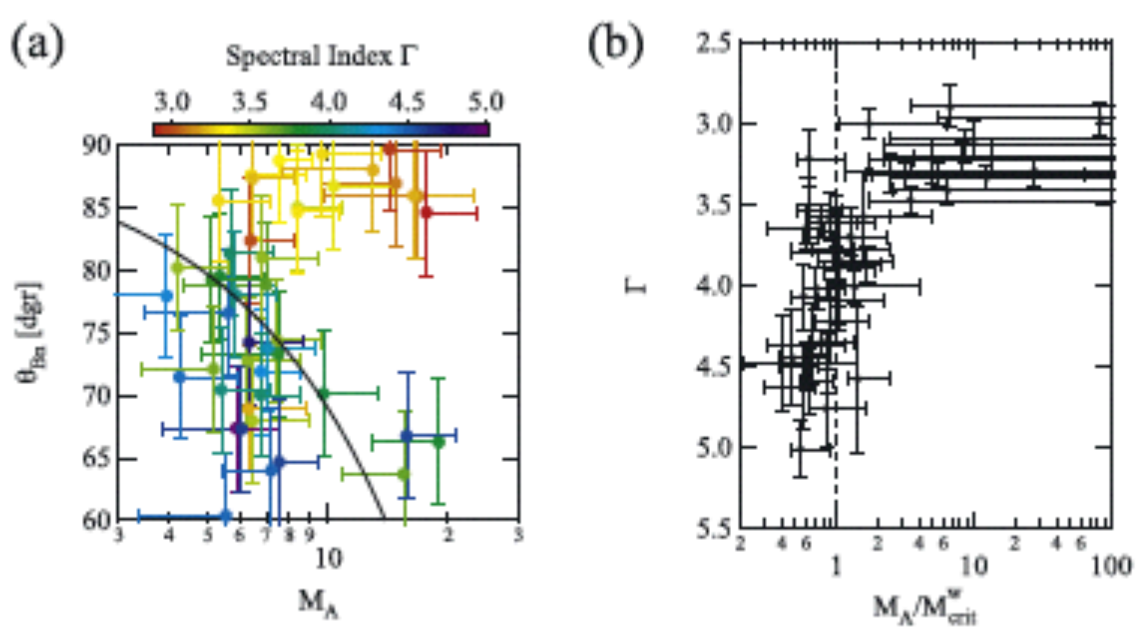

Oka et al 2006, Geotail, Earth's bow shock

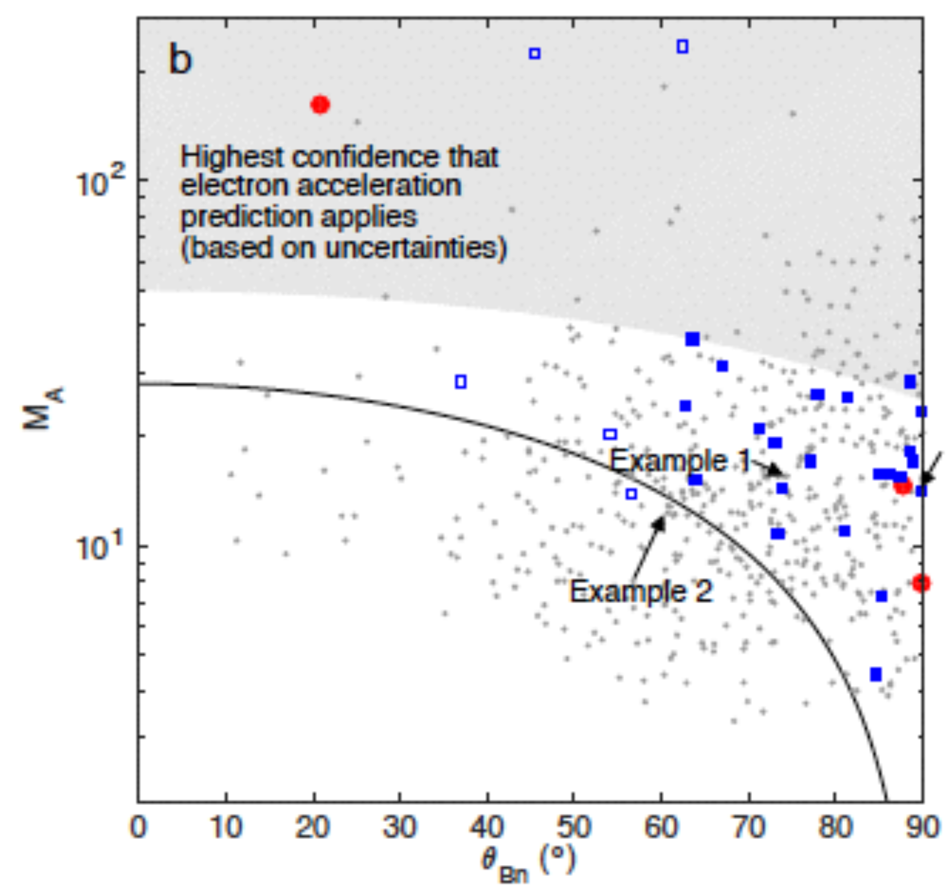

Masters et al 2016, Cassini, Saturns's bow shock

Summary and conclusions

- electron injections needs to be understood in the nonrelativistic regime
- at high Mach number quasi-perpendicular shocks in cold plasmas (low-beta plasmas) shock-surfing acceleration (SSA) seems to be a viable process for initial electron injection
- subsequent pre-acceleration may proceed through shock-drift acceleration (SDA) and be followed by scattering on upstream self-generated waves
- world is 3D, but 2D experiments can still be elucidating
- multi-dimensional and large-scale effects need also to be taken into account in kinetic modeling - need for exa-scale computing